Modeling of microgrids—from fundamental physics to phasors and voltage sources

Johannes Schiffer[a,*], Daniele Zonetti[b], Romeo Ortega[b], Aleksandar Stanković[c], Tevfik Sezi[d], Jörg Raisch[a,e]

[a] *Technische Universität Berlin, Einsteinufer 11, 10587 Berlin, Germany*
[b] *Laboratoire des Signaux et Systémes, École Supérieure d'Electricité (SUPELEC), Gif-sur-Yvette 91192, France*
[c] *Tufts University, Medford, MA 02155, USA*
[d] *Siemens AG, Smart Grid Division, Energy Automation, Humboldtstr. 59, 90459 Nuremberg, Germany*
[e] *Max-Planck-Institut für Dynamik komplexer technischer Systeme, Sandtorstr. 1, 39106 Magdeburg, Germany*

arXiv:1505.00136v1 [cs.SY] 1 May 2015

Abstract

Microgrids are an increasingly popular class of electrical systems that facilitate the integration of renewable distributed generation units. Their analysis and controller design requires the development of advanced (typically model-based) techniques naturally posing an interesting challenge to the control community. Although there are widely accepted reduced order models to describe the dynamic behavior of microgrids, they are typically presented without details about the reduction procedure—hampering the understanding of the physical phenomena behind them. The present paper aims to provide a complete modular model derivation of a three-phase inverter-based microgrid. Starting from fundamental physics, we present detailed dynamical models of the main microgrid components and clearly state the underlying assumptions which lead to the standard reduced model representation with inverters represented as controllable voltage sources, as well as static network interconnections and loads.

Keywords: Microgrid modeling, microgrid analysis, smart grid applications, inverters

1. Introduction

1.1. Motivation

It is a widely accepted fact that fossil-fueled thermal power generation highly contributes to greenhouse gas emissions [63, 95]. In addition, a growing stream of scientific results [47, 42, 90] substantiates claims that greenhouse gas emissions are a key driver for climate change and global warming. As a consequence, many countries have agreed to reduce their greenhouse gas emissions.

Apart from a reduction of energy consumption, *e.g.*, through an increase in efficiency, one possibility to reduce greenhouse gas emissions is to shift the energy production from fossil-fueled plants towards renewable sources [95]. Therefore, the worldwide use of renewable energies has increased significantly in recent years [92, 95].

Unlike fossil-fueled thermal power plants, most renewable power plants are relatively small in terms of their generation power. An important consequence of this smaller size is that most renewable power plants are connected to the low voltage (LV) and medium voltage (MV) levels. Such generation units are commonly denoted as distributed generation (DG) units [1]. In addition, most renewable DG units are interfaced to the network via AC inverters. The physical characteristics of such power electronic devices largely differ from the characteristics of synchronous generators (SGs), which are the standard generating units in existing power systems. Hence, different control and operation strategies are needed in networks with a large amount of renewable DG units [37, 95].

1.2. The microgrid concept

One potential solution to facilitate the integration of large shares of renewable DG units are microgrids [57, 43, 37, 51]. A microgrid gathers a combination of generation units, loads and energy storage elements at distribution or sub-transmission level into a locally controllable system, which can be operated either in grid-connected mode or in islanded mode, *i.e.*, in a completely isolated manner from the main transmission system. The microgrid concept has been identified as a key component in future electrical networks [30, 58].

Many new control problems arise for this type of networks. Their satisfactory solution requires the development of advanced model-based controller design techniques that often go beyond the classical linearization-based nested-loop proportional-integral (PI) schemes. This situation

*Corresponding author J. Schiffer. Tel. +49-30-314-23573. Fax +49-30-314-21137.

Email addresses: schiffer@control.tu-berlin.de (Johannes Schiffer), zonetti@lss.supelec.fr (Daniele Zonetti), ortega@lss.supelec.fr (Romeo Ortega), astankov@ece.tufts.edu (Aleksandar Stanković), tevfik.sezi@arcor.de (Tevfik Sezi), raisch@control.tu-berlin.de (Jörg Raisch)

has, naturally, attracted the attention of the control community as it is confronted with some new challenging control problems of great practical interest.

It is clear that to carry out this task it is necessary to develop a procedure for assembling mathematical models of a microgrid that reliably capture the fundamental aspects of the problem. Such models have been developed by the power systems and electronics communities and their pertinence has been widely validated in simulations and applications [20, 49, 74, 67]. However, these are reduced or simplified, *i.e.*, linearized, models that are typically presented without any reference to the reduction procedure—hampering the understanding of the physical phenomena behind them.

1.3. Existing literature

For the purposes of this paper, previous work on microgrid modeling can be broadly categorized into two classes. The first class focusses on modeling and control of inverter-interfaced DG units in microgrid applications, but the model derivation is restricted to individual DG units and the current and power flows between different units are not considered explicitly [37, 74, 49, 103, 77, 38, 10, 11]. The second class discusses models of microgrids including electrical network interactions, but the model derivation is based on linearization (*i.e.*, the so-called small-signal model) [50, 74, 67]. Furthermore, this class of modeling is often tied to specific network control schemes, such as droop control [20, 74] or to specific test networks [49, 50, 67, 66]. Building on this previous work and in a survey-like manner, the present paper brings both aforementioned classes together to formulate a generic modular model of a microgrid.

In this paper, we use model reduction via a time-scale separation together with the subsequent derivation of the well-known power flow equations, which is a standard procedure in SG-based networks [96]. It has also been employed for microgrids in [65, 64, 76, 62]. However, neither reference provides a detailed model derivation for inverter-interfaced units. Also, the analysis in [65, 64] is restricted to an AC microgrid consisting of two inverters connected via a resistive-inductive line and two local resistive-inductive loads, while the modeling procedure of the present paper applies to networks with generic topology and arbitrary number of units.

1.4. About the paper

The present paper is an attempt to provide a guideline for control engineers attracted by this emerging application to quantify the dynamics of the main components of a three-phase inverter-based microgrid and assess the validity of different models used in the power literature. Starting from fundamental physics, we present their detailed dynamical models and clearly state the underlying assumptions which lead to the standard reduced model representation with inverters represented as controllable voltage sources, as well as static network interconnections and loads used in most of the available work on microgrid control design and analysis [89, 83, 2, 69, 27].

We focus on purely inverter-based networks, since inverter-interfaced units are the main new elements in microgrids compared to traditional power systems. For modeling of traditional electro-mechanical SG-based DG units, the reader is referred to standard textbooks on power systems [55, 63, 5].

The main contributions of the paper are summarized as follows.

- Provide a detailed model derivation of a microgrid based on fundamental physics.
- Answer the question, when an inverter can be modeled as a controllable AC voltage source and depict the necessary underlying model assumptions.
- Show that the usual power flow equations can be obtained from a network with dynamic line models via a suitable coordinate transformation (called dq-transformation) together with a singular perturbation argument.
- By combining the two latter contributions, recover the reduced-order microgrid model currently widely used in the literature.

We emphasize that the aim of the present paper is not to give an overarching justification for the final (simplified) model, but to provide a comprehensive overview of the modeling procedure for main microgrid components together with their dynamics, as well as of the main necessary assumptions, which allow the reduction of model complexity. Which of the presented models (if any) is appropriate for a specific control design and analysis cannot be established in general, but has to be decided by the user. Any model used in simulation and analysis necessarily involves certain assumptions. Therefore, it is of great importance that the user is aware of the pertinence of the employed model to appropriately assess the implications of a model-based analysis.

1.5. Control goals in microgrids

For the sake of completeness, we briefly review control goals in microgrids. At the present, the following are considered to be among the most relevant control objectives in microgrids [30, 57, 37, 43, 51, 34, 38]: frequency stability, voltage stability, operational compatibility of inverter-interfaced and SG-interfaced units, desired power sharing in steady-state, seamless switching from grid-connected to islanded-mode and vice-versa, robustness with respect to uncertainties and optimal dispatch.

Some of these problems have been addressed in recent work within the control community, *e.g.*, frequency and voltage stability [88, 89, 83, 93, 24, 2, 69, 85, 86, 27], secondary control [10, 88, 11, 27, 87] or optimal dispatch

[27, 14, 13, 41]. Compared to the model derived in the present paper, most of the aforementioned work is conducted under certain additional simplifying assumptions, such as constant voltage amplitudes, identical DG unit dynamics, lossless or identical lines.

The remainder of the paper is structured as follows. Basic preliminaries, such as definitions and transformations in power systems are given in Section 2. The microgrid concept is presented in Section 3. A detailed dynamical model of a microgrid is derived in Section 4. In particular, common operation modes of inverter-interfaced units are discussed therein. The model reduction yielding models of inverters as AC voltage sources and phasorial power flow equations is conducted in Section 5. The paper is wrapped-up with some conclusions in Section 6.

Notation. We define the sets $\mathbb{R}_{\geq 0} := \{x \in \mathbb{R} | x \geq 0\}$, $\mathbb{R}_{>0} := \{x \in \mathbb{R} | x > 0\}$ and $\mathbb{S} := [0, 2\pi)$. For a set $\mathcal{V}$, let $|\mathcal{V}|$ denote its cardinality. For a set of, possibly unordered, positive natural numbers $\mathcal{V} = \{l, k, \ldots, n\}$, the short-hand $i \sim \mathcal{V}$ denotes $i = l, k, \ldots, n$. Given a positive integer n, we use $\underline{0}_n$ to denote the vector of all zeros, $\mathbb{1}_n$ the vector with all ones and $\mathbf{I}_n$ the $n \times n$ identity matrix. Let $x = \mathrm{col}(x_1, \ldots, x_n) \in \mathbb{C}^n$ denote a column vector with entries $x_i \in \mathbb{C}$. Whenever clear from the context, we simply write $x = \mathrm{col}(x_i) \in \mathbb{C}^n$. The 2-norm of a vector $x \in \mathbb{C}^n$ is denoted by $\|x\|_2 = \sqrt{|x_1|^2 + \ldots + |x_n|^2}$. Let $\mathrm{diag}(a_i) \in \mathbb{C}^{n \times n}$ denote a diagonal matrix with entries $a_i \in \mathbb{C}$. Let j denote the imaginary unit. The conjugate transpose of a matrix $A \in \mathbb{C}^{n \times n}$ is denoted by A^*. For a function $f : \mathbb{R}^n \to \mathbb{R}$, ∇f denotes the transpose of its gradient. The operator $\otimes$ denotes the Kronecker product.

2. Preliminaries and basic definitions

2.1. Symmetric AC three-phase signals

Definition 2.1. *[25] A signal $x : \mathbb{R}_{\geq 0} \to \mathbb{R}$ is said to be an AC signal if it satisfies the following conditions*

1. *it is periodic with period $T \in \mathbb{R}_{>0}$,* i.e.*,*

$$x(t) = x(t + nT), \quad \forall n \in \mathbb{N}, \quad \forall t \geq 0,$$

2. *its arithmetic mean is zero,* i.e.*,*

$$\int_t^{t+T} x(\tau) d\tau = 0 \quad \forall t \geq 0.$$

Definition 2.2. *A signal $x : \mathbb{R}_{\geq 0} \to \mathbb{R}^3$ is said to be a three-phase AC signal if it is of the form*

$$x_{ABC} = col(x_A, x_B, x_C),$$

where $x_A : \mathbb{R}_{\geq 0} \to \mathbb{R}$, $x_B : \mathbb{R}_{\geq 0} \to \mathbb{R}$ and $x_C : \mathbb{R}_{\geq 0} \to \mathbb{R}$ are AC signals.

A special kind of three-phase AC signals are symmetric AC three-phase signals, defined below.

Definition 2.3. *[4, Chapter 2] A three-phase AC signal $x_{abc} : \mathbb{R}_{\geq 0} \to \mathbb{R}^3$ is said to be symmetric if it can be described by*

$$x_{abc}(t) = \begin{bmatrix} x_a(t) \\ x_b(t) \\ x_c(t) \end{bmatrix} = A(t) \begin{bmatrix} \sin(\delta(t)) \\ \sin(\delta(t) - \frac{2\pi}{3}) \\ \sin(\delta(t) + \frac{2\pi}{3}) \end{bmatrix},$$

where $A : \mathbb{R}_{\geq 0} \to \mathbb{R}_{\geq 0}$ is called the amplitude and $\delta : \mathbb{R}_{\geq 0} \to \mathbb{S}$ is called the phase angle of the signal.

Clearly, from the preceding definition, a symmetric three-phase AC signal x_{abc} can be described completely by two signals: its angle δ and its amplitude A.[1]

Definition 2.4. *[4, Chapter 2] A three-phase AC signal is said to be asymmetric if it is not symmetric.*

Definition 2.5. *[45, Chapter 3] A three-phase AC electrical system is said to be symmetrically configured if a symmetrical feeding voltage yields a symmetrical current and vice versa.*

Definition 2.6. *[45, Chapter 3] A three-phase AC power system is said to be operated under symmetric conditions if it is symmetrically configured and symmetrically fed.*

Examples of symmetric and asymmetric three-phase AC signals[2] are given in Fig. 1.

Remark 2.7. The terms "balanced" and "unbalanced" are frequently used as synonyms of "symmetric", respectively "asymmetric" in the literature [4, 34].

Remark 2.8. Three-phase electrical power systems consist of three main conductors in parallel. Each of these conductors carries an AC current. A three-phase system can be arranged in Δ- or Y-configuration. The latter is also called wye-configuration. Frequently, in a system with Y-configuration an additional fourth grounded neutral conductor is used to reduce transient overvoltages and to carry asymmetric currents [34, Chapter 2]. Such systems are typically called three-phase four-wire systems. Most three-phase power systems are four-wire Y-connected systems with grounded neutral conductor [34, Chapter 2]. However, it can be shown that, under symmetric operating conditions, this fourth wire does not carry any current and can therefore be neglected [34, Chapter 2].

[1] To simplify notation the time argument of all signals is omitted, whenever clear from the context. The same applies to the definition of signals, *i.e.*, a signal $x : \mathbb{R}_{\geq 0} \to \mathbb{R}$, is defined equally as $x \in \mathbb{R}$, whenever clear from the context.

[2] In this paper only AC systems and signals are considered. Therefore, the qualifier AC is dropped from now on.

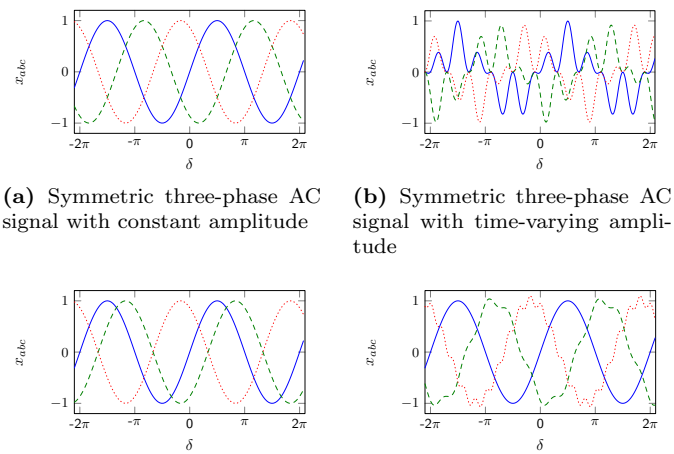

(a) Symmetric three-phase AC signal with constant amplitude

(b) Symmetric three-phase AC signal with time-varying amplitude

(c) Asymmetric three-phase AC signal with phases not shifted equally by $\frac{2\pi}{3}$

(d) Asymmetric three-phase AC signal resulting of an asymmetric superposition of a symmetric signal with signals oscillating at higher frequencies

Figure 1: Symmetric and asymmetric AC three-phase signals. The lines correspond to x_a '—', x_b '- -', x_c '· · ·'.

2.2. The dq0-transformation

An important coordinate transformation known as $dq0$-transformation in the literature [71, 70, 5, 63, 92, 6, 103] is introduced.

Definition 2.9. *[5, Chapter 4], [63, Chapter 11] Let $x : \mathbb{R}_{\geq 0} \to \mathbb{R}^3$ and $\varrho : \mathbb{R}_{\geq 0} \to \mathbb{S}$. Consider the mapping $T_{dq0} : \mathbb{S} \to \mathbb{R}^{3\times 3}$,*

$$T_{dq0}(\varrho) := \sqrt{\frac{2}{3}} \begin{bmatrix} \cos(\varrho) & \cos(\varrho - \frac{2}{3}\pi) & \cos(\varrho + \frac{2}{3}\pi) \\ \sin(\varrho) & \sin(\varrho(t) - \frac{2}{3}\pi) & \sin(\varrho + \frac{2}{3}\pi) \\ \frac{\sqrt{2}}{2} & \frac{\sqrt{2}}{2} & \frac{\sqrt{2}}{2} \end{bmatrix}. \tag{2.1}$$

Then, $f_{dq0} : \mathbb{R}^3 \times \mathbb{S} \to \mathbb{R}^3$,

$$f_{dq0}(x(t), \varrho(t)) = T_{dq0}(\varrho(t))x(t) \tag{2.2}$$

is called $dq0$-transformation.

Note that the mapping (2.1) is unitary, *i.e.*, $T_{dq0}^\top = T_{dq0}^{-1}$. From a geometrical point of view, the $dq0$-transformation is a concatenation of two rotational transformations, see [70] for further details. The variables in the transformed coordinates are often denoted by $dq0$-variables.

The $dq0$-transformation offers various advantages when analyzing and working with power systems and is therefore widely used in applications [70, 5, 4, 92, 103]. For example, the $dq0$-transformation permits, through appropriate choice of ϱ, to map three-phase AC signals to constant signals, *i.e.*, to transform periodic orbits into constant equilibria. This simplifies the control design and analysis in power systems, which is the main reason why the transformation (2.2) is introduced in the present case. In addition, the transformation (2.2) exploits the fact that, in a power system operated under symmetric conditions, a three-phase signal can be represented by two quantities. To see this, let $x_{abc} : \mathbb{R}_{\geq 0} \to \mathbb{R}^3$ be a symmetric three-phase signal with amplitude $A : \mathbb{R}_{\geq 0} \to \mathbb{R}_{\geq 0}$ and phase angle $\theta : \mathbb{R}_{\geq 0} \to \mathbb{S}$, as in Definition 2.3. Applying the mapping (2.1) with some angle $\varrho : \mathbb{R}_{\geq 0} \to \mathbb{S}$ to x_{abc} yields

$$x_{dq0} = \begin{bmatrix} x_d \\ x_q \\ x_0 \end{bmatrix} = T_{dq0}(\varrho)x_{abc} = \sqrt{\frac{3}{2}}A \begin{bmatrix} \sin(\theta - \varrho) \\ \cos(\theta - \varrho) \\ 0 \end{bmatrix}.$$

Hence, $x_0 = 0$ for all $t \geq 0$. Therefore and as in this work only symmetric three-phase signals are considered, it is convenient to introduce the mapping $T_{dq} : \mathbb{S} \to \mathbb{R}^{2\times 3}$,

$$T_{dq}(\varrho) := \sqrt{\frac{2}{3}} \begin{bmatrix} \cos(\varrho) & \cos(\varrho - \frac{2}{3}\pi) & \cos(\varrho + \frac{2}{3}\pi) \\ \sin(\varrho) & \sin(\varrho - \frac{2}{3}\pi) & \sin(\varrho + \frac{2}{3}\pi) \end{bmatrix}, \tag{2.3}$$

which, when applied to the symmetric three-phase signal x_{abc} defined above, yields

$$x_{dq} = \begin{bmatrix} x_d \\ x_q \end{bmatrix} = T_{dq}(\varrho)x_{abc} = \sqrt{\frac{3}{2}}A \begin{bmatrix} \sin(\theta - \varrho) \\ \cos(\theta - \varrho) \end{bmatrix}.$$

In the following, x_{dq} are referred to as the dq-coordinates of x_{abc}. Note that $x_{abc} = T_{dq}(\varrho)^\top x_{dq}$.

Remark 2.10. There are several variants of the mapping (2.1) available in the literature. They may differ from the mapping (2.1) in the order of the rows and the sign of the entries in the second row of the matrix given in (2.1), see [5, 6, 103]. However, all representations are equivalent in the sense that they can all be represented by T_{dq0} as given in (2.1) by choosing an appropriate angle ϱ and, possibly, rearranging the row order of the matrix T_{dq0}. The same applies to the mapping T_{dq} given in (2.3). Since—with a slightly different scaling factor—this transformation was first introduced by Robert H. Park in 1929 [71] it is also often called Park transformation [92, Appendix A].

2.3. Instantaneous power

Power is one of the most important quantities in control, monitoring and operation of electrical networks. The first theoretical contributions to the definition of the power flows in an AC network date back to the early 20th century. However, these first definitions are restricted to sinusoidal steady-state conditions and based on the root-mean-square values of currents and voltages. As a consequence, these definitions of electric power are not well-suited for the purposes of network control under time-varying operating conditions [4].

The extension of the definition of electrical power to time-varying operating conditions is called "instantaneous power theory" in the power system and power electronics community [4, 92]. The development of this theory already begun in the 1930s with the study of active and non-active components of currents and voltages [32]. Among others, relevant contributions are [16, 21, 3, 100, 22, 72, 53].

Today, it is widely agreed by researchers and practitioners [100, 72, 92] that the definitions of instantaneous power proposed in [3] and contained in [4] are well-suited for describing the power flows in three-phase three-wire systems and symmetric three-phase four-wire systems. However, a proper definition of instantaneous power in asymmetric three-phase four-wire systems with nonzero neutral current and voltage is still an open (and controversial) field of research [23, 4, 7, 92]. A good overview of the research history on instantaneous power theory is given in [92, Appendix B].

Consider a symmetric three-phase voltage, respectively current, given by

$$v_{abc} = \sqrt{2}V \begin{bmatrix} \sin(\theta) \\ \sin(\theta - \frac{2\pi}{3}) \\ \sin(\theta + \frac{2\pi}{3}) \end{bmatrix}, \quad i_{abc} = \sqrt{2}I \begin{bmatrix} \sin(\varphi) \\ \sin(\varphi - \frac{2\pi}{3}) \\ \sin(\varphi + \frac{2\pi}{3}) \end{bmatrix}, \tag{2.4}$$

where $\theta : \mathbb{R}_{\geq 0} \to \mathbb{S}$ and $\varphi : \mathbb{R}_{\geq 0} \to \mathbb{S}$ are the phase angles and $\sqrt{2}V : \mathbb{R}_{\geq 0} \to \mathbb{R}_{\geq 0}$, respectively $\sqrt{2}I : \mathbb{R}_{\geq 0} \to \mathbb{R}_{\geq 0}$, the amplitudes of the respective three-phase signal. As shown in Section 2.2, applying the transformation (2.3) to the signals given in (2.4) yields

$$\begin{aligned} v_{dq} &= \begin{bmatrix} V_d \\ V_q \end{bmatrix} = \sqrt{3}V \begin{bmatrix} \sin(\theta - \varrho) \\ \cos(\theta - \varrho) \end{bmatrix}, \\ i_{dq} &= \begin{bmatrix} I_d \\ I_q \end{bmatrix} = \sqrt{3}I \begin{bmatrix} \sin(\varphi - \varrho) \\ \cos(\varphi - \varrho) \end{bmatrix}. \end{aligned} \tag{2.5}$$

Based on the preceding discussion, the following definitions of instantaneous active, reactive and apparent power under symmetric, but not necessarily steady-state, conditions are used in this work. The definitions are based on [3, 4], in which they are given in $\alpha\beta$-coordinates. For the purpose of the present paper, it is more convenient to equivalently define the instantaneous powers in dq-coordinates.

Definition 2.11. *Let $v_{dq}(t)$ and $i_{dq}(t)$ be given by (2.5). The instantaneous three-phase active power is defined as*

$$P(t) := v_{dq}^\top(t) i_{dq}(t) = V_d(t)I_d(t) + V_q(t)I_q(t).$$

The instantaneous three-phase reactive power is defined as

$$Q(t) := v_{dq}^\top(t) \begin{bmatrix} 0 & 1 \\ -1 & 0 \end{bmatrix} i_{dq}(t) = V_d(t)I_q(t) - V_q(t)I_d(t).$$

Finally, the instantaneous three-phase (complex) apparent power is defined as

$$S(t) := P(t) + jQ(t).$$

From the above definition, straight-forward calculations together with standard trigonometric identities yield

$$\begin{aligned} P(t) &= 3V(t)I(t)\cos(\theta(t) - \varphi(t)), \\ Q(t) &= 3V(t)I(t)\sin(\theta(t) - \varphi(t)). \end{aligned}$$

It follows that whenever v_{abc} and i_{abc} given in (2.4) possess constant amplitudes, as well as the same frequency, i.e., $\dot{\theta} = \dot{\varphi}$, all quantities P, Q and S are constant. Moreover, then the given definitions of power are in accordance with the conventional definitions of power in a symmetric steady-state [36, 4, 34]. For further information on definitions and physical interpretations of instantaneous power, also under asymmetric conditions, the reader is referred to [100, 72, 28, 101, 4, 92].

Since this work is mainly concerned with dynamics of generation units, all powers are expressed in "Generator Convention" [34, Chapter 2]. That is, delivered active power is positive, while absorbed active power is negative. Furthermore, capacitive reactive power is counted positively and inductive reactive power is counted negatively.

3. The microgrid concept

Microgrids have attracted a wide interest in different research and application communities over the last decade [88, 43, 74]. However, the term "microgrid" is not uniformly defined in the literature [57, 43, 37, 51, 19, 34]. Based on [37, 43], the following definition of an AC microgrid is employed in this paper.

Definition 3.1. *An AC electrical network is said to be an AC microgrid if it satisfies the following conditions.*

1. *It is a connected subset of the LV or MV distribution system of an AC electrical power system.*
2. *It possesses a single point of connection to the remaining electrical power system. This point of connection is called point of common coupling (PCC).*
3. *It gathers a combination of generation units, loads and energy storage elements.*
4. *It possesses sufficient generation and storage capacity to supply most of its loads autonomously during at least some period of time.*
5. *It can be operated either connected to the remaining electrical network or as an independent island network. The first operation mode is called grid-connected mode and the second operation mode is called islanded, stand-alone or autonomous mode.*
6. *In islanded mode, it is a locally controllable system, that is frequency, voltage and power can be actively controlled within the microgrid.*
7. *In grid-connected mode, it behaves as a single controllable generator or load from the viewpoint of the remaining electrical system.*

According to Definition 3.1, the main components in a microgrid are DG units, loads and energy storage elements. Typical DG units in microgrids are renewable DG units, such as photovoltaic (PV) units, wind turbines, fuel cells (FCs), as well as microturbines or reciprocating engines in combination with SGs. The latter two can either be powered with biofuels or fossil fuels [59, 34].

Typical loads in a microgrid are residential, commercial and industrial loads [57, 51, 59]. It is also foreseen to categorize the loads in a microgrid with respect to their priorities, *e.g.*, critical and non-critical loads. This enables load shedding as a possible operation option in islanded mode [57, 59].

Finally, storage elements play a key-role in microgrid operation [59, 34]. They are especially useful in balancing the power fluctuations of intermittent renewable sources and, hence, to contribute to network control. Possible storage elements are, *e.g.*, batteries, flywheels or supercapacitors. The combination of renewable DGs and storage elements is also an important assumption for the inverter models derived in this paper. An illustration of an exemplary microgrid is given in Fig. 2.

Most of the named DG and storage units are either DC sources (PV, FC, batteries) or are often operated at variable or high-speed frequency (wind turbines, microturbines, flywheels). Therefore, they have to be connected to an AC network via AC or DC-AC inverters [37, 92]. For ease of notation, such devices are simply called "inverters" in the following. Overviews on existing test-sites and experimental microgrids around the globe are provided in the survey papers [43, 8, 59, 73, 40].

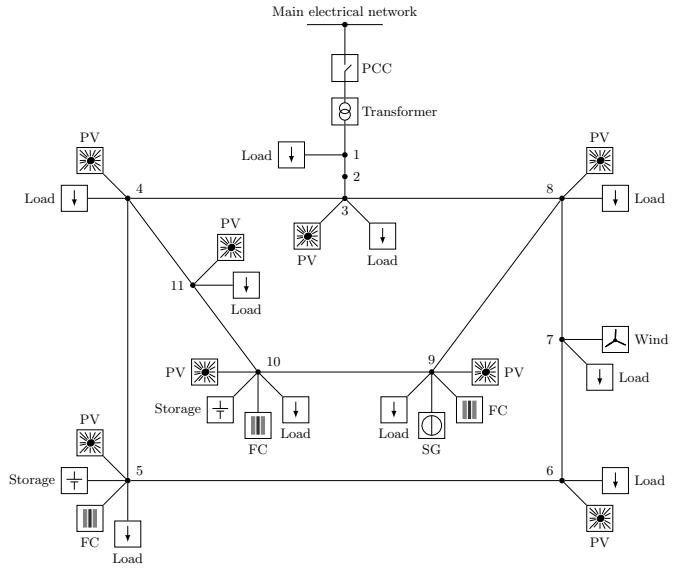

Figure 2: Schematic representation of a microgrid. The microgrid is composed of several DG units, loads and storage devices. The DG units are inverter-interfaced photovoltaic (PV), fuel cell (FC) and wind power plants. In addition, a power generation unit is connected to the network via a synchronous generator (SG). The point of connection of the microgrid to the main network is called point of common coupling (PCC).

Remark 3.2. While not comprised in Definition 3.1, true island power systems are sometimes also called microgrids in the literature [43]. This can be justified by the fact that island power systems operating with a large share of renewable energy sources face similar technical challenges as microgrids. Nevertheless, an island power system differs from a microgrid in that it cannot be frequently connected to and disconnected from a larger electrical network [37].

Remark 3.3. Microgrids can also be implemented as DC systems [78, 79, 56]. Definition 3.1 can easily be adapted to this scenario by removing the property "frequency control" in point 6. Recent reviews of the main differences and challenges for AC and DC microgrids are given in [98, 73, 48].

4. Modeling of inverter-based microgrids

As outlined in the previous section, an AC microgrid is a spatially small power system the main components of which are renewable DG units, loads and energy storage elements interconnected through a network of AC transmission lines and transformers. Furthermore, most renewable DG and storage units are interconnected to the network via inverters. As a consequence, fundamental network control actions, such as frequency or voltage control, have to be performed by inverter-interfaced units. This fact represents a fundamental difference to the operation of conventional power systems, where mainly SG units are responsible for network control. Therefore and since the modeling of SGs is a well-covered topic in the literature [55, 5, 63], we focus in the following on microgrids with purely inverter-interfaced DG and storage units. Also, it is straight-forward to incorporate SG-based units into the microgrid model presented hereafter.

In line with these considerations, an inverter-based microgrid can be represented by an undirected graph[3] $\mathcal{G} = (\mathcal{N}, \mathcal{E})$, in which—similarly to [31]—nodes represent voltage buses, edges represent dynamic power lines and the topology of the network is fully described by the incidence matrix $\mathcal{B}$. In the present case, we further assume that the set of nodes $\mathcal{N}$ can be partitioned into two subsets $\mathcal{N}_I$ and $\mathcal{N}_R$, associated to inverter and load nodes respectively. We next proceed as follows. First, we provide a description of the basic functionality and common operation modes of inverters that are instrumental for the modeling. Thereafter, we present models of inverters—depending on their mode of operation—loads, power lines and transformers. The section is concluded by combining the individual models to an overall representation of an inverter-based microgrid. To enhance readability, the subindex i, preceded by a comma when necessary, denotes in the sequel the elements corresponding to the i-th subsystem.

[3] An undirected graph of order n is a tuple $\mathcal{G} := (\mathcal{V}, \mathcal{E})$, where $\mathcal{V} := \{n_1, \ldots, n_n\}$ is the set of nodes and $\mathcal{E} \subseteq \mathcal{V} \times \mathcal{V}$, $\mathcal{E} := \{e_1, \ldots, e_m\}$ is the set of undirected edges. The l-th edge connecting nodes i and k is denoted as $e_l = (i, k) = (k, i)$. By associating an arbitrary ordering to the edges, the node-edge incidence matrix $\mathcal{B} \in \mathbb{R}^{|\mathcal{V}| \times |\mathcal{E}|}$ is defined element wise as $b_{il} = 1$, if node i is the sink of the l-th edge e_l, $b_{il} = -1$, if i is the source of e_l and $b_{il} = 0$ otherwise. For further information on graph theory, the reader is referred to, *e.g.*, [35] and references therein.

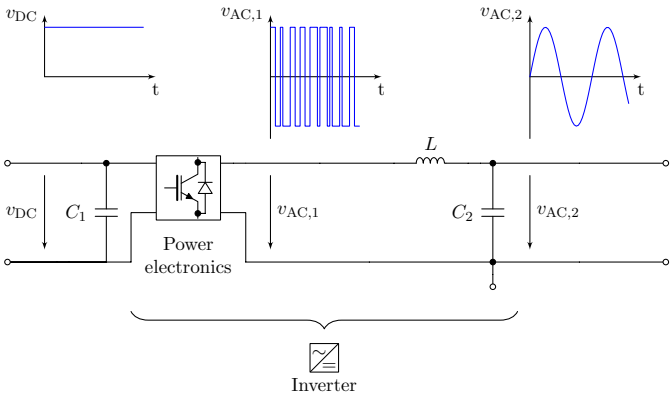

Figure 3: Schematic representation of a DC-AC voltage conversion by a DC-AC inverter. The DC signal $v_{\mathrm{DC}} : \mathbb{R}_{\geq 0} \to \mathbb{R}$ on the left side is converted into an AC signal via power semiconductor devices. The generated AC signal $v_{\mathrm{AC},1} : \mathbb{R}_{\geq 0} \to \mathbb{R}^3$ at the output of the power electronics is not sinusoidal. Therefore, an LC filter is connected in series with the power electronics to obtain an approximately sinusoidal ouput voltage $v_{\mathrm{AC},2} : \mathbb{R}_{\geq 0} \to \mathbb{R}^3$ with low harmonic content.

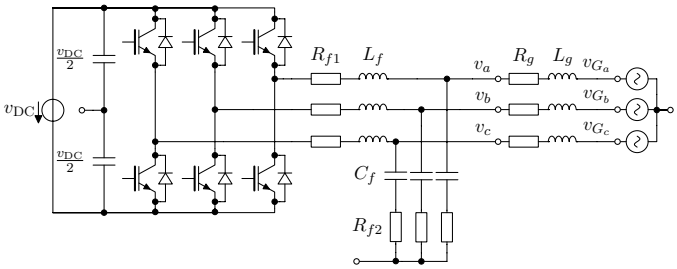

Figure 4: Typical circuit of a two-level three-phase inverter with LC output filter to convert a DC into a three-phase AC voltage. The inverter is constructed with insulated-gate bipolar transistors (IGBTs) and antiparallel diodes. The DC voltage is denoted by $v_{\mathrm{DC}} : \mathbb{R}_{\geq 0} \to \mathbb{R}$, the three-phase AC voltage generated by the inverter with $v_{abc} : \mathbb{R}_{\geq 0} \to \mathbb{R}^3$, $v_{abc} = \mathrm{col}(v_a, v_b, v_c)$ and the three-phase grid-side AC voltage by $v_G : \mathbb{R}_{\geq 0} \to \mathbb{R}^3$, $v_G = \mathrm{col}(v_{G_a} v_{G_b}, v_{G_c})$. The components of the output filter are an inductance $L_f \in \mathbb{R}_{>0}$, a capacitance $C_f \in \mathbb{R}_{>0}$ and two resistances $R_{f_1} \in \mathbb{R}_{>0}$, respectively $R_{f_2} \in \mathbb{R}_{>0}$. Typically, the resistance $R_g \in \mathbb{R}_{>0}$ and the inductance $L_g \in \mathbb{R}_{>0}$ represent a transformer or an output impedance. At the open connectors denoted by "**o**" the circuit can be grounded if desired.

4.1. Basic functionality and common operations of an inverter

Recall that inverters are key components of microgrids. Therefore, this section is dedicated to the model derivation of an inverter in a microgrid. The basic functionality of an inverter is illustrated in Fig. 3. The main elements of inverters are power semiconductor devices [29, 68]. An exemplary basic hardware topology of the electric circuit of a two-level three-phase inverter constructed with insulated-gate bipolar transistors (IGBTs) and antiparallel diodes is shown in Fig. 4. The conversion process from DC to AC is usually achieved by adjusting the on- and off-times of the transistors. These on- and off-time sequences are typically determined via a modulation technique, such as pulse-width-modulation [29, 68]. To improve the quality of the AC waveform, *e.g.*, to reduce the harmonics, the generated AC signal is typically processed through a low-pass filter constructed with LC elements. Further information on the hardware design of inverters and related controls is given in [29, 68, 103].

In microgrids, two main operation modes for inverters can be distinguished [98, 77]: grid-forming and grid-feeding mode. The latter is sometimes also called grid-following mode [51] or PQ control [61], whereas the first is also referred to as voltage source inverter (VSI) control [61]. The main characteristics of these two different operation modes are as follows [61, 51, 98, 77].

1. Grid-forming mode (also: VSI control).
   The inverter is controlled in such way that its output voltage can be specified by the designer. This is typically achieved via a cascaded control scheme consisting of an inner current control and an outer voltage control as shown in Fig. 5, based on [77]. The feedback signal of the current control loop is the current through the filter inductance, while the feedback signal of the voltage control loop is the inverter output voltage $v_{abc} : \mathbb{R}_{\geq 0} \to \mathbb{R}^3$. The inner loop of the control cascade is not necessary to control the output voltage of the inverter and can hence also be omitted. Nevertheless, it is often included to improve the control performance.
2. Grid-feeding mode (also: grid-following mode, PQ control).
   The inverter is operated as power source, *i.e.*, it provides a pre-specified amount of active and reactive power to the grid. The active and reactive power setpoints are typically provided by a higher-level control or energy management system, see [77, 14, 41]. Also in this case, a cascaded control scheme is usually implemented to achieve the desired closed-loop behavior of the inverter, as illustrated in Fig. 6. As in the case of a grid-forming inverter, the inner control loop is a current control the feedback signal of which is the current through the filter inductance. However, the outer control loop is not a voltage, but rather a power (or, sometimes, a current) control. The feedback signals of the power control are the active and reactive power provided by the inverter.

In both aforementioned operation modes, the current and voltage control loops are, in general, designed with the objectives of rejecting high frequency disturbances, enhancing the damping of the output $LC(L)$ filter and providing harmonic compensation [75, 12, 67, 74]. Furthermore, nowadays, most inverter-based DG units, such as PV or wind plants, are operated in grid-feeding mode [77]. However, grid-forming units are essential components in AC power systems, since they are responsible for frequency and voltage regulation in the network. Therefore, in microgrids with a large share of renewable inverter-based DG units, grid-forming capabilities often also have to be pro-

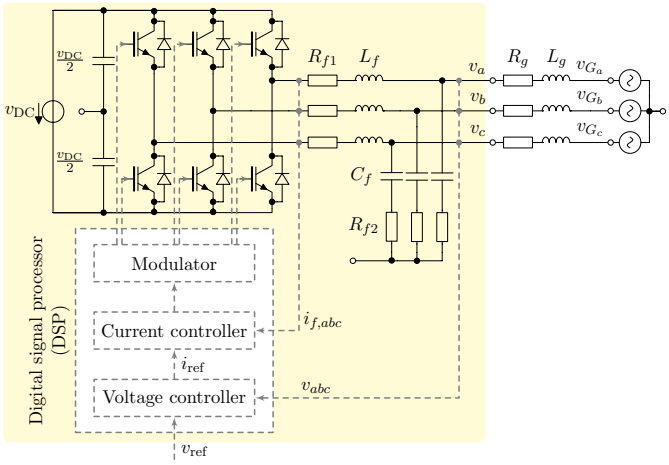

Figure 5: Schematic representation of an inverter operated in grid-forming mode based on [77]. Bold lines represent electrical connections, while dashed lines represent signal connections. The current through the filter inductance is denoted by $i_{f,abc} : \mathbb{R}_{\geq 0} \to \mathbb{R}^3$ and the inverter output voltage by $v_{abc} : \mathbb{R}_{\geq 0} \to \mathbb{R}^3$. Both quantities are fed back to a cascaded control consisting of an outer voltage and an inner current control. The reference signal $v_{\text{ref}} : \mathbb{R}_{\geq 0} \to \mathbb{R}^3$ for the voltage controller is set by the designer, respectively a higher-level control. The IGBTs of the inverter are then controlled via signals generated by a modulator. The control structure can also be reduced to a pure voltage control.

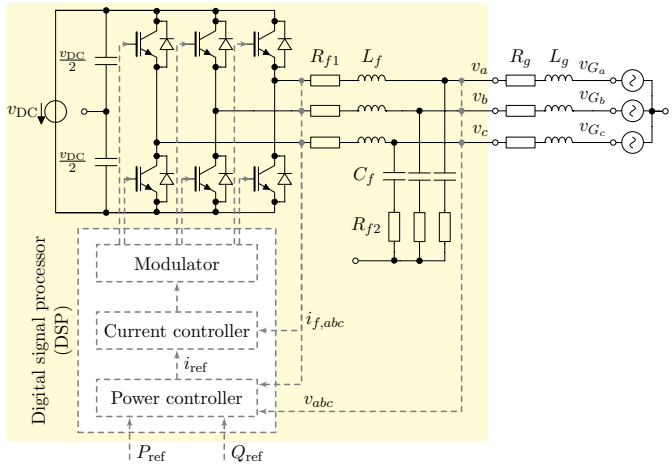

Figure 6: Schematic representation of an inverter operated in grid-feeding mode based on [77]. Bold lines represent electrical connections, while dashed lines represent signal connections. As in Fig. 5, the current through the filter inductance is denoted by $i_{f,abc} : \mathbb{R}_{\geq 0} \to \mathbb{R}^3$ and the inverter output voltage by $v_{abc} : \mathbb{R}_{\geq 0} \to \mathbb{R}^3$. In grid-feeding mode, both quantities are fed back to a cascaded control consisting of an outer power and an inner current controller. The reference active and reactive powers $P_{\text{ref}} \in \mathbb{R}$, respectively $Q_{\text{ref}} \in \mathbb{R}$, are set by the designer or a higher-level control.

vided by inverter-interfaced sources [61, 51].

Remark 4.1. Some authors [98, 77] also introduce a third operation mode for inverters called grid-supporting mode. Nevertheless, this last category is not necessary to classify typical operation modes of inverters in microgrids in the context of this work, since grid-supporting inverters are grid-forming inverters equipped with an additional outer control-loop to determine the reference output voltage. Such outer control-loops are, *e.g.*, the usual droop controls [17, 38]. Therefore, the term "grid-supporting inverter" is not used in the following.

Remark 4.2. In addition to the two control schemes introduced above, there also exist other approaches to operate inverters in microgrid applications. For example, [9, 97, 102] propose to design the inverter control based on the model of an SG with the aim of making the inverter mimic as closely as possible the behavior of an SG. However, to the best of the authors' knowledge, these approaches do not consider additional aspects, such as harmonic compensation or improved damping. Furthermore, they are not as commonly used as the control schemes shown in Fig. 5 and Fig. 6.

4.2. Modeling of grid-forming inverters

A suitable model of a grid-forming inverter for the purpose of control design and stability analysis of microgrids is derived. There are many control schemes available to operate an inverter in grid-forming mode, such as PI control in *dq*-coordinates [74], proportional resonant control [33, 91] or repetitive control [99, 46] among others. An overview of the most common control schemes with an emphasis on H_∞ repetitive control is given in [103]. For a comparison of different control schemes, the reader is referred to [60]. The assumption below is made for the model derivation.

Assumption 4.3. *Whenever an inverter connects an intermittent renewable generation source, it is equipped with a fast-reacting storage.*

Assumption 4.3 implies that the inverter can increase and decrease its power output within a certain range. This is necessary if the inverter should be capable of providing a fully controllable voltage also when interfacing an intermittent renewable DG unit to the network. Furthermore, since the storage element is assumed to be fast-reacting, the DC-side dynamics can be neglected in the model.

Due to the large variety of available control schemes, it is difficult to determine a standard closed-loop model of an inverter operated in grid-forming mode together with its inner control and output filter. Therefore, the approach taken in this work is to represent such a system as a generic dynamical system. Note that the operation of the IGBTs of an inverter occurs typically at very high switching frequencies (2-20 kHz) compared to the network frequency (45-65 Hz). It is therefore common practice [61, 37, 74, 67, 18] to model an inverter in network studies with continuous dynamics by using the so-called averaged switch modeling technique [29, 18], *i.e.*, by averaging the internal inverter voltage and current over a suitably chosen time interval such as one switching period.

It is convenient to partition the set $\mathcal{N}_I$ into two subsets, *i.e.*, $\mathcal{N}_I = \mathcal{N}_1 \cup \mathcal{N}_2$, such that $\mathcal{N}_1$ contains all nodes asso-

ciated to grid-forming inverters and $\mathcal{N}_2$ contains those associated to grid-feeding inverters. Consider a grid-forming inverter located at the i-th node of a given microgrid, *i.e.*, $i \in \mathcal{N}_1$. Denote its three-phase symmetric output voltage by $v_{abc,i} : \mathbb{R}_{\geq 0} \to \mathbb{R}^3$ with phase angle $\alpha_i : \mathbb{R}_{\geq 0} \to \mathbb{S}$ and amplitude $\sqrt{\frac{2}{3}} V_i : \mathbb{R}_{\geq 0} \to \mathbb{R}_{\geq 0}$, *i.e.*,

$$v_{abc,i} = \sqrt{\frac{2}{3}} V_i \begin{bmatrix} \sin(\alpha_i) \\ \sin(\alpha_i - \frac{2}{3}\pi) \\ \sin(\alpha_i + \frac{2}{3}\pi) \end{bmatrix}.$$

Furthermore, denote by $\omega_i := \dot{\alpha}_i$ the frequency of the voltage $v_{abc,i}$. Denote the state signal of the inverter with its inner control and output filter by $x_i : \mathbb{R}_{\geq 0} \to \mathbb{R}^m$, its input signal by $v_{\mathrm{ref},i} : \mathbb{R}_{\geq 0} \to \mathbb{R}^3$ and its interconnection port signals by $v_{abc,i}$ and $i_{abc,i} : \mathbb{R}_{\geq 0} \to \mathbb{R}^3$, see Fig. 5. Let $f_i : \mathbb{R}^m \times \mathbb{R}^3 \times \mathbb{R}^3 \to \mathbb{R}^m$ and $h_i : \mathbb{R}^m \times \mathbb{R}^3 \to \mathbb{R}^3$ denote continuously differentiable functions and ν_i denote a nonnegative real constant. Then, the closed-loop inverter dynamics with inner control and output filter can be represented in a generic manner as

$$\begin{aligned} \nu_i \gamma_i \dot{x}_i &= f_i(x_i, v_{\mathrm{ref},i}, i_{abc,i}), \\ v_{abc,i} &= h_i(x_i, v_{\mathrm{ref},i}), \end{aligned} \tag{4.1}$$

where the positive real constant γ_i denotes the time-drift due to the clock drift of the processor used to operate the inverter, see [84] for further details. Note that $i_{abc,i}$ represents a disturbance for the inner control system.

One key objective in microgrid applications is to design suitable higher-level controls to provide a reference voltage $v_{\mathrm{ref},i}$ for the system (4.1) [38]. Within the hierarchical control scheme discussed, *e.g.*, in [39, 38] this next higher control level corresponds to the primary control layer of a microgrid. Let $z_i : \mathbb{R}_{\geq 0} \to \mathbb{R}^p$ denote the state signal of this higher-level control system, $u_i : \mathbb{R}_{\geq 0} \to \mathbb{R}^q$ its input signal and $v_{\mathrm{ref},i}$ its output signal. Furthermore, let $g_i : \mathbb{R}^p \times \mathbb{R}^q \to \mathbb{R}^p$ and $w_i : \mathbb{R}^p \times \mathbb{R}^q \to \mathbb{R}^3$ be continuously differentiable functions. Then, the outer control system of the inverter can be described by

$$\begin{aligned} \gamma_i \dot{z}_i &= g_i(z_i, u_i), \\ v_{\mathrm{ref},i} &= w_i(z_i, u_i). \end{aligned} \tag{4.2}$$

Combining (4.1) and (4.2) yields the overall inverter dynamics for the i-th node, $i \in \mathcal{N}_1$,

$$\begin{aligned} \gamma_i \dot{z}_i &= g_i(z_i, u_i), \\ \nu_i \gamma_i \dot{x}_i &= f_i(x_i, w_i(z_i, u_i), i_{abc,i}), \\ v_{abc,i} &= h_i(x_i, w_i(z_i, u_i)). \end{aligned} \tag{4.3}$$

4.3. Modeling of grid-feeding inverters and loads

As discussed in Section 4.1, grid-feeding inverters are typically operated as current or power sources. In order to achieve such behavior, the control methods employed to design the inner control loops of grid-forming inverters (see Section 4.2) can equivalently be applied to operate inverters in grid-feeding mode. The current or power reference values are typically provided by a higher-level control, *e.g.*, a maximum power point tracker (MPPT) [77].

We define the set $\mathcal{N}_\ell := \mathcal{N}_2 \cup \mathcal{N}_R$ that contains the nodes associated to grid-feeding inverters and loads. As done for the model of a grid-forming inverter in (4.3), let $x_{\ell,i} : \mathbb{R}_{\geq 0} \to \mathbb{R}^r$ denote the state signal, $v_{abc,i} : \mathbb{R}_{\geq 0} \to \mathbb{R}^3$ and $i_{abc,i} : \mathbb{R}_{\geq 0} \to \mathbb{R}^3$ denote the interconnection port signals, $f_{\ell,i} : \mathbb{R}^r \times \mathbb{R}^3 \to \mathbb{R}^r$ and $h_{\ell,i} : \mathbb{R}^r \times \mathbb{R}^3 \to \mathbb{R}^3$ denote continuously differentiable functions and κ_i denote a nonnegative real constant. We assume then a generic dynamic model of the form

$$\begin{aligned} \kappa_i \dot{x}_{\ell,i} &= f_{\ell,i}(x_{\ell,i}, i_{abc,i}), \\ v_{abc,i} &= h_{\ell,i}(x_{\ell,i}, i_{abc,i}), \end{aligned} \tag{4.4}$$

for any node $i \in \mathcal{N}_\ell$. In addition to grid-feeding inverters, the model (4.4) can equivalently represent impedance (*e.g.*, R parallel to L), current- or power-controlled loads. Furthermore, a large variety of other load behaviors can be modeled by (4.4). We refer the reader to [55, 94] for further details on load modeling.

4.4. Modeling of power lines and transformers

We recall that the set of power lines and transformers interconnecting the different network nodes $i \sim \mathcal{N}$ is given by $\mathcal{E}$. The main purpose of the present paper is to provide a structured modeling procedure for microgrids. For ease of presentation, we make the following assumption.

Assumption 4.4. *All power lines and transformers can be represented by symmetric three-phase RL elements.*

In light of Assumption 4.4 and to ease presentation, we solely use the term power lines to refer to the network interconnections in the following sections. Also, note that it is straight-forward to extent the modeling approach presented hereafter to more detailed power line models and to DG units interfaced to the network via SGs.

Associate an arbitrary ordering to the power lines $e_l \sim \mathcal{E}$ and to each power line $e_l \in \mathcal{E}$ a line current $i_{L,l} : \mathbb{R}_{\geq 0} \to \mathbb{R}^3$. With Assumption 4.4, consider a three-phase symmetric power line $e_l \in \mathcal{E}$ connecting a pair of nodes $(i, k) \in \mathcal{N} \times \mathcal{N}$. Each phase of the power line e_l is composed of a constant ohmic resistance $R_l \in \mathbb{R}_{>0}$ in series with a constant inductance $L_l \in \mathbb{R}_{>0}$, and the voltage drop across the line is given by

$$v_{L,l} := v_{abc,i} - v_{abc,k}.$$

Denote the state of the l-th line by $x_{L,l} := i_{L,l}$ and its interconnection port variables by $v_{L,l}$ and $i_{L,l}$. Then, the model of the l-th line $e_l \in \mathcal{E}$ is given by

$$\begin{aligned} L_l \dot{x}_{L,l} &= -R_l x_{L,l} + v_{L,l} \\ i_{L,l} &= x_{L,l}. \end{aligned} \tag{4.5}$$

It is convenient to define the aggregated nodal voltages and currents

$$v_{abc} := \mathrm{col}(v_{abc,i}) \in \mathbb{R}^{3|\mathcal{N}|},\ i_{abc} := \mathrm{col}(i_{abc,i}) \in \mathbb{R}^{3|\mathcal{N}|},$$

the aggregated line voltages and currents

$$v_L := \mathrm{col}(v_{L,l}) \in \mathbb{R}^{3|\mathcal{E}|}, \quad i_L := \mathrm{col}(i_{L,l}) \in \mathbb{R}^{3|\mathcal{E}|},$$

as well as the matrices

$$L := \mathrm{diag}(L_l) \in \mathbb{R}^{|\mathcal{E}|\times|\mathcal{E}|}, \quad R := \mathrm{diag}(R_l) \in \mathbb{R}^{|\mathcal{E}|\times|\mathcal{E}|}.$$

The three-phase interconnection laws can be obtained by following the approach used in [31], where Kirchhoff's current and voltage laws (KCL and KVL) are expressed in relation to the node-edge incidence matrix $\mathcal{B}$, *i.e.*,

$$i_{abc} = \mathcal{B} \otimes \mathbf{I}_3 i_L, \qquad \mathcal{B}^\top \otimes \mathbf{I}_3 v_{abc} = v_L.$$

Hence, the dynamical system representing the network is given by

$$\begin{aligned} L \otimes \mathbf{I}_3 \dot{x}_L &= -R \otimes \mathbf{I}_3 x_L + \mathcal{B}^\top \otimes \mathbf{I}_3 v_{abc} \\ i_{abc} &= \mathcal{B} \otimes \mathbf{I}_3 x_L \end{aligned} \tag{4.6}$$

We next transform the model (4.6) into dq-coordinates by means of the transformation T_{dq} introduced in (2.3). This coordinate transformation is instrumental for the model reduction carried out in Section 5. Let

$$\phi := \mathrm{mod}_{2\pi}\left(\omega^{\mathrm{com}} t\right) \in \mathbb{S}, \tag{4.7}$$

where the operator[4] $\mathrm{mod}_{2\pi}$ is added to respect the topology of the torus. Applying the transformation T_{dq} with transformation angle ϕ to the signals $v_{abc,i}$ and $i_{abc,i}$, $i \sim \mathcal{N}$, gives

$$\hat{v}_{dq,i} := T_{dq}(\phi) v_{abc,i} = \begin{bmatrix} \hat{V}_{d,i} \\ \hat{V}_{q,i} \end{bmatrix},\ \hat{i}_{dq,i} := T_{dq}(\phi) i_{abc,i} = \begin{bmatrix} \hat{I}_{d,i} \\ \hat{I}_{q,i} \end{bmatrix},$$

where the superscript "$\hat{\cdot}$" is introduced to denote signals in dq-coordinates with respect to the angle ϕ. This notation is used in the subsequent section, where a reduced-order model of a microgrid is derived by using several dq-transformation angles. Furthermore, following standard notation in power systems, the constant $\dot{\phi} = \omega^{\mathrm{com}}$ is referred to as the rotational speed of the common reference frame. Likewise, the signal $x_{L,l}$ in (4.5) becomes

$$\hat{x}_{L,dq,l} := T_{dq}(\phi) x_{L,abc,l} = \begin{bmatrix} \hat{X}_{L,d,l} \\ \hat{X}_{L,q,l} \end{bmatrix}.$$

Note that

$$\begin{aligned} \dot{\hat{x}}_{L,dq,l} &= \dot{T}_{dq}(\phi) x_{L,l} + T_{dq}(\phi) \dot{x}_{L,l} \\ &= \omega^{\mathrm{com}} \begin{bmatrix} -\hat{X}_{L,q,l} \\ \hat{X}_{L,d,l} \end{bmatrix} + T_{dq}(\phi) \dot{x}_{L,l}. \end{aligned}$$

[4]The operator $\mathrm{mod}_{2\pi} : \mathbb{R} \to [0, 2\pi)$, is defined as follows: $y = \mathrm{mod}_{2\pi}\{x\}$ yields $y = x - k2\pi$ for some integer k, such that $y \in [0, 2\pi)$.

Hence, (4.5) reads in dq-coordinates as

$$L_l \dot{\hat{x}}_{L,dq,l} = -R_l \hat{x}_{L,dq,l} + L_l \omega^{\mathrm{com}} \begin{bmatrix} -\hat{X}_{L,q,l} \\ \hat{X}_{L,d,l} \end{bmatrix} + \hat{v}_{dq,l}. \tag{4.8}$$

By defining the aggregated nodal voltages and currents in dq-coordinates

$$\hat{v}_{dq} := \mathrm{col}(\hat{v}_{dq,i}) \in \mathbb{R}^{2|\mathcal{N}|},\ \hat{i}_{dq} := \mathrm{col}(\hat{i}_{dq,i}) \in \mathbb{R}^{2|\mathcal{N}|},$$

the aggregated line voltage and currents in dq-coordinates

$$\hat{v}_{L,dq} := \mathrm{col}(\hat{v}_{L,dq,l}) \in \mathbb{R}^{2|\mathcal{E}|}, \quad \hat{x}_{L,dq} := \mathrm{col}(\hat{i}_{L,dq,l}) \in \mathbb{R}^{2|\mathcal{E}|},$$

as well as the matrix

$$\mathcal{X} := \mathrm{diag}\left(L_l \omega^{\mathrm{com}} \begin{bmatrix} 0 & -1 \\ 1 & 0 \end{bmatrix} \right) \in \mathbb{R}^{2|\mathcal{E}|\times 2|\mathcal{E}|},$$

(4.6) becomes in dq-coordinates

$$\begin{aligned} L \otimes \mathbf{I}_2 \dot{\hat{x}}_{L,dq} &= (-R \otimes \mathbf{I}_2 + \mathcal{X}) \hat{x}_{L,dq} + \mathcal{B}^\top \otimes \mathbf{I}_2 \hat{v}_{dq} \\ \hat{i}_{dq} &= \mathcal{B} \otimes \mathbf{I}_2 \hat{x}_{L,dq}. \end{aligned} \tag{4.9}$$

4.5. Overall model

By defining the state vectors $z \in \mathbb{R}^{p|\mathcal{N}_1|}$, $x \in \mathbb{R}^{m|\mathcal{N}_1|}$, $x_\ell \in \mathbb{R}^{r|\mathcal{N}_\ell|}$, the input $u \in \mathbb{R}^{q|\mathcal{N}_1|}$, the matrices

$$\begin{aligned} &\Gamma := \mathrm{diag}(\gamma_i) \in \mathbb{R}^{|\mathcal{N}_1|\times|\mathcal{N}_1|},\ \mathsf{V} := \mathrm{diag}(\nu_i) \in \mathbb{R}^{|\mathcal{N}_1|\times|\mathcal{N}_1|}, \\ &K := \mathrm{diag}(\kappa_i) \in \mathbb{R}^{|\mathcal{N}_2|\times|\mathcal{N}_2|}, \end{aligned}$$

and combining (4.3), (4.4) and (4.9), the overall microgrid model (see Fig. 7) is given by the differential equations

$$\begin{aligned} \left[\Gamma \otimes \mathbf{I}_{p|\mathcal{N}_1|}\right] \dot{z} &= g(z, u) \\ \left[\mathsf{V}\Gamma \otimes \mathbf{I}_{m|\mathcal{N}_1|}\right] \dot{x} &= f(x, w(z, u), i_{abc}) \\ \left[K \otimes \mathbf{I}_{r|\mathcal{N}_\ell|}\right] \dot{x}_\ell &= f_\ell(x_\ell, i_{abc}) \\ \left[L \otimes \mathbf{I}_2\right] \dot{\hat{x}}_{L,dq} &= (-R \otimes \mathbf{I}_2 + \mathcal{X}) \hat{x}_{L,dq} + \mathcal{B}^\top \otimes \mathbf{I}_2 \hat{v}_{dq}, \end{aligned} \tag{4.10}$$

together with the algebraic relations

$$\begin{aligned} i_{abc} &= \mathcal{B} \otimes \mathbf{I}_3 x_L = \mathcal{B} \otimes T_{dq}(\phi)^\top \hat{x}_{L,dq}, \\ v_{abc,i} &= h_i(x_i, w_i(z_i, u_i)), \\ v_{abc,k} &= h_{\ell,k}(x_{\ell,k}, i_{abc,k}), \\ \hat{v}_{dq} &= \mathbf{I}_{|\mathcal{N}|} \otimes T_{dq}(\phi) v_{abc}, \quad i \sim \mathcal{N}_1, \quad k \sim \mathcal{N}_\ell. \end{aligned} \tag{4.11}$$

5. To phasors and voltage sources via time-scale separation

For the purpose of deriving an interconnected network model suitable for network stability analysis, it is customary to make the following assumptions on (4.10), (4.11). Let ϵ be a small positive real constant.

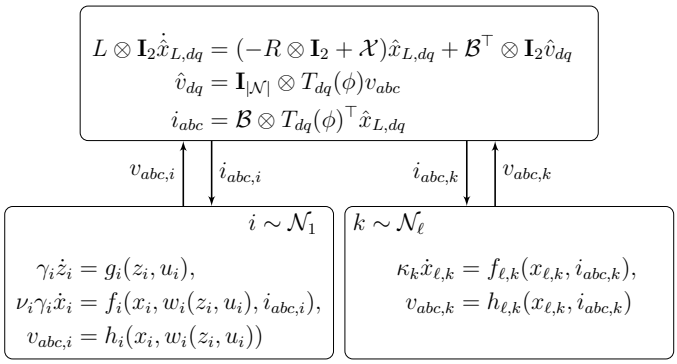

Figure 7: Port-based representation of an inverter based-microgrid modeled by (4.10), (4.11).

Assumption 5.1. *$\nu_i < \epsilon$ in (4.3), $i \sim \mathcal{N}_1$. Therefore, $\dot{x}_i(t) = \underline{0}_m$ for all $t \geq 0$. Furthermore, $v_{abc,i} = w_i(z_i, u_i)$, $i \sim \mathcal{N}_1$.*

Assumption 5.2. *$\kappa_i < \epsilon$ in (4.4), $k \sim \mathcal{N}_\ell$. Therefore, $\dot{x}_{\ell,k}(t) = \underline{0}_r$ for all $t \geq 0$. Furthermore, the power balance at each node $k \in \mathcal{N}_\ell$ can be described by a ZIP model [55], i.e.,*

$$\begin{aligned} P_k(\hat{v}_{dq,k}, \hat{i}_{dq,k}) &= -\left(a_{P,k}\|\hat{v}_{dq,k}\|_2^2 + b_{P,k}\|\hat{v}_{dq,k}\|_2 + c_{P,k}\right), \\ &:= P_k^*(\|\hat{v}_{dq,k}\|_2), \\ Q_k(\hat{v}_{dq,k}, \hat{i}_{dq,k}) &= -\left(a_{Q,k}\|\hat{v}_{dq,k}\|_2^2 + b_{Q,k}\|\hat{v}_{dq,k}\|_2 + c_{Q,k}\right) \\ &:= Q_k^*(\|\hat{v}_{dq,k}\|_2), \end{aligned}$$

where $a_{P,k}$, $b_{P,k}$, $c_{P,k}$, $a_{Q,k}$, $b_{Q,k}$ and $c_{Q,k}$ are real constants and $P_k(\hat{v}_{dq,k}, \hat{i}_{dq,k})$ and $Q_k(\hat{v}_{dq,k}, \hat{i}_{dq,k})$ are calculated as given in Definition 2.11.

Assumption 5.3. *$L < \epsilon \mathbf{I}_{|\mathcal{E}|}$ in (4.9). Therefore, $\dot{\hat{x}}_{L,dq}(t) = \underline{0}_{2|\mathcal{E}|}$ for all $t \geq 0$.*

Assumption 5.1 is equivalent to the assumption that the inner current and voltage controllers track the voltage and current references instantaneously and exactly. Usually, the current and voltage controllers in (4.1) (see also Fig. 5) are designed such the resulting closed-loop system (4.1) has a very large bandwidth compared to the control system located at the next higher control level represented by (4.2) [61, 20, 67]. If this time-scale separation is followed in the design of the system (4.3), the first part of Assumption 5.1 can be mathematically formalized by invoking the singular perturbation theory [52, Chapter 11], [54]. The second part of Assumption 5.1 expresses the fact that the inner control system (4.1) is assumed to track the reference $v_{\text{ref},i} = w_i(z_i, u_i)$ exactly, independently of the disturbance $i_{abc,i}$. Typical values for the bandwidth of (4.1) reported in [67, 74] are in the range of $400 - 600$ Hz, while those of (4.2) are in the range of $2 - 10$ Hz.

Assumption 5.2 implies that the dynamics of loads and grid-feeding units can be neglected. This assumption is also frequently employed in microgrid and power system stability studies, where loads are often modeled as either constant impedance (Z), constant current (I) or constant power loads (P) or a combination of them (ZIP) [55, 94]. Similarly, grid-feeding units with positive active power injection are represented by setting $a_{P,k} = a_{Q_k} = 0$ and $b_{P,k}$ or $c_{P,k}$ to negative values. The values for $b_{Q,k}$ and $c_{Q,k}$ should be chosen in dependency of the reactive power contribution of the unit.

Assumption 5.3 is standard in power system analysis [55, 36, 80, 5, 63, 34]. The usual justification of Assumption 5.3 is that the line dynamics evolve on a much faster time-scale than the dynamics of the generation sources. In the present case, Assumption 5.3 is justified whenever Assumption 5.1 is employed, since the line dynamics (4.9) are typically at least as fast as those of the internal inverter controls (4.1), see, *e.g.*, [74]. Again, Assumption 5.3 can be mathematically formalized by invoking singular perturbation arguments [52, Chapter 11], [54].

Under Assumption 5.1, the model of each grid-forming inverter (4.3) reduces to

$$\begin{aligned} \gamma_i \dot{z}_i &= g_i(z_i, u_i), \\ v_{abc,i} &= w_i(z_i, u_i), \quad i \sim \mathcal{N}_1. \end{aligned} \tag{5.1}$$

The model (5.1) represents the inverter as an AC voltage source, the amplitude and frequency of which can be defined by the designer. The system (5.1) is a very commonly used model of a grid-forming inverter in microgrid control design and analysis [61, 37, 51, 83]. The model simplification from (4.3) to (5.1) is illustrated in Figure 8.

Furthermore, often a particular structure of (5.1) is used in the literature [88, 89, 81, 83, 2, 69]. As discussed in Section 2.1, a symmetric three-phase voltage can be completely described by its phase angle and its amplitude. In addition, it is usually preferred to control the frequency of the inverter output voltage, instead of the phase angle. Hence, a suitable model of the inverter at the i-th node is given by [83, 81]

$$\begin{aligned} \gamma_i \dot{\alpha}_i &= \omega_i = u_i^\delta, \\ V_i &= u_i^{\mathrm{V}}, \\ v_{abc,i} &= v_{abc,i}(\alpha_i, V_i), \end{aligned} \tag{5.2}$$

where $u_i^\delta : \mathbb{R}_{\geq 0} \to \mathbb{R}$ and $u_i^V : \mathbb{R}_{\geq 0} \to \mathbb{R}$ are control signals.

Usually, it is also assumed that the active and reactive power output is measured and processed through a filter to obtain the power components corresponding to the fundamental frequency [74, 20, 67]

$$\begin{aligned} \gamma_i \tau_{P_i} \dot{P}_i^m &= -P_i^m + P_i, \\ \gamma_i \tau_{P_i} \dot{Q}_i^m &= -Q_i^m + Q_i. \end{aligned} \tag{5.3}$$

Here, P_i and Q_i are the active and reactive power injections of the inverter, $P_i^m : \mathbb{R}_{\geq 0} \to \mathbb{R}$ and $Q_i^m : \mathbb{R}_{\geq 0} \to \mathbb{R}$ their measured values and $\tau_{P_i} \in \mathbb{R}_{>0}$ is the time constant of the low pass filter.

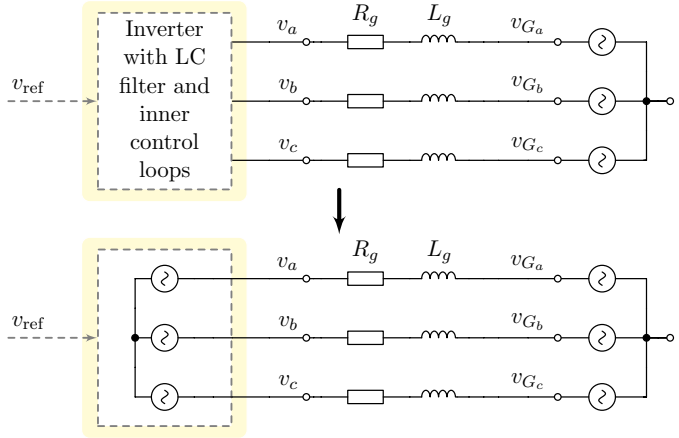

Figure 8: Simplified representation of an inverter operated in grid-forming mode as ideal controllable voltage source. Bold lines represent electrical connections, while dashed lines represent signal connections.

Note that whenever the particular form (5.2), (5.3) of (4.2) is considered and the measured and filtered power signals are used as feedback signals in the controls u_i^δ, respectively u_i^{V}, then the bandwidth of the overall control system is limited by the bandwidth of the measurement filter. Hence, if $\tau_{P_i} \gg \nu_i$, then Assumption 5.1 is justified.

With Assumption 5.2, (4.4) can be represented by the algebraic relation

$$\begin{aligned} P_k(\hat{v}_{dq,k}, \hat{i}_{dq,k}) &= P_k^*(\|\hat{v}_{dq,k}\|_2), \\ Q_k(\hat{v}_{dq,k}, \hat{i}_{dq,k}) &= Q_k^*(\|\hat{v}_{dq,k}\|_2), \quad k \sim \mathcal{N}_\ell. \end{aligned} \tag{5.4}$$

Finally, under Assumption 5.3, the network interconnections (4.9) are also static and given by

$$\hat{i}_{dq} = \mathcal{B} \otimes \mathbf{I}_2 \left(R \otimes \mathbf{I}_2 - \mathcal{X}\right)^{-1} \mathcal{B}^\top \otimes \mathbf{I}_2 \hat{v}_{dq}. \tag{5.5}$$

In the following, a more compact representation of (5.2) - (5.5) is derived. To this end, it is convenient to recall that α_i is the angle of the voltage at the i-th node with initial condition α_{0_i}, $i \sim \mathcal{N}$ and define

$$\delta_i := \alpha_{0_i} + \int_0^t (\dot{\alpha}_i - \omega^{\text{com}}) d\tau \in \mathbb{S}, \quad i \sim \mathcal{N}. \tag{5.6}$$

Let $\varpi : \mathbb{R}_{\geq 0} \to \mathbb{S}$ and consider the mapping $T_\delta : \mathbb{S} \to \mathbb{R}^{2\times 2}$,

$$T_\delta(\varpi) := \begin{bmatrix} \cos(\varpi) & \sin(\varpi) \\ -\sin(\varpi) & \cos(\varpi) \end{bmatrix}. \tag{5.7}$$

Note that, with δ_i defined in (5.6),

$$\alpha_i - \delta_i = \text{mod}_{2\pi}\left(\omega^{\text{com}} t\right) = \phi, \quad i \sim \mathcal{N},$$

and that straightforward algebraic manipulations yield

$$T_{dq}(\phi) = T_\delta(\delta_i) T_{dq}(\alpha_i).$$

Hence, by construction,

$$\hat{v}_{dq,i} = T_{dq}(\phi) v_{abc,i} = T_\delta(\delta_i) T_{dq}(\alpha_i) v_{abc,i} = T_\delta(\delta_i) V_i \begin{bmatrix} 0 \\ 1 \end{bmatrix}, \tag{5.8}$$

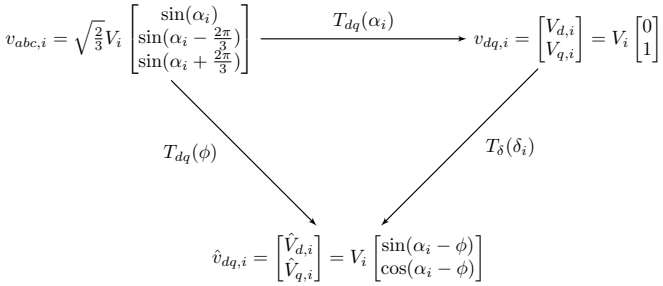

Figure 9: Illustration of the different coordinate frames used to derive the model of an electrical network given in (5.15). The signal $v_{abc,i} : \mathbb{R}_{\geq 0} \to \mathbb{R}^3$ denotes the three-phase voltage at the i-th bus with phase angle $\alpha_i : \mathbb{R}_{\geq 0} \to \mathbb{S}$ and amplitude $V_i : \mathbb{R}_{\geq 0} \to \mathbb{R}_{\geq 0}$, $i \sim \mathcal{N}_I$. The mappings T_{dq} and T_δ are given in (2.3), respectively (5.7). The angle $\delta_i : \mathbb{R}_{\geq 0} \to \mathbb{S}$ is defined in (5.6). Note that, by construction, $\alpha_i - \delta_i = \text{mod}_{2\pi}\left(\omega^{\text{com}} t\right) = \phi$, where the real constant ω^{com} denotes the speed of the common dq-reference frame.

which makes it convenient to define

$$v_{dq,i} := \begin{bmatrix} V_{d,i} \\ V_{q,i} \end{bmatrix} = V_i \begin{bmatrix} 0 \\ 1 \end{bmatrix}, \quad i \sim \mathcal{N}. \tag{5.9}$$

The variables $v_{dq,i}$ are referred to as local dq-coordinates of $v_{abc,i}$ in the following. The relation between $v_{abc,i}$, $\hat{v}_{dq,i}$ and $v_{dq,i}$ is illustrated in Fig. 9.

It is convenient to represent (5.8) in the complex plane

$$\hat{V}_{qd,i} := \hat{V}_{q,i} + j\hat{V}_{d,i} = (\cos(\delta_i) + j\sin(\delta_i)) V_{qd,i} = e^{j\delta_i} V_{qd,i}, \tag{5.10}$$

where $V_{qd,i} = V_{q,i} + jV_{d,i}$, $i \sim \mathcal{N}$. Equivalently, let

$$\hat{I}_{qd,i} := \hat{I}_{q,i} + j\hat{I}_{d,i} = e^{j\delta_i} I_{qd,i} \tag{5.11}$$

and define

$$\begin{aligned} \hat{V}_{qd} &:= \hat{V}_q + j\hat{V}_d \in \mathbb{C}^{|\mathcal{N}|}, \quad \hat{I}_{qd} := \hat{I}_q + j\hat{I}_d \in \mathbb{C}^{|\mathcal{N}|}, \\ V_{qd} &:= V_q + jV_d \in \mathbb{C}^{|\mathcal{N}|}, \quad I_{qd} := I_q + jI_d \in \mathbb{C}^{|\mathcal{N}|}. \end{aligned} \tag{5.12}$$

Then, with $X := \text{diag}(X_l) = \text{diag}(L_l \omega^{\text{com}}) \in \mathbb{R}^{|\mathcal{E}|\times|\mathcal{E}|}$, we can rewrite (5.5) as

$$\hat{I}_{qd} = \mathcal{B}\left(R + jX\right)^{-1} \mathcal{B}^\top \hat{V}_{qd}. \tag{5.13}$$

Note that the reactances $X_l = L_l \omega^{\text{com}}$ are calculated at the frequency ω^{com}, which, under the made assumptions, should be chosen as the (constant) synchronous frequency of the network—denoted by $\omega^s \in \mathbb{R}$ in the following[5]. Typically, $\omega^s \in 2\pi[45, 65]$ rad/s.

Remark 5.4. The form (5.12) is a very popular representation and these complex quantities are often denoted as phasors [5, 103]. Furthermore, by using Euler's formula

[5] Under the made assumptions, (5.5) is the equilibrium of the "fast" line dynamics (4.8) [52, Chapter 11]. Hence, in order for the currents $\hat{i}_{dq}$ and voltages $\hat{v}_{dq}$ to be constant in steady-state, ω^{com} has to be chosen equivalently to the synchronous steady-state network frequency.

[44], (5.12) can also be rewritten in polar form. Note, however, that, unlike, *e.g.*, [5, 103], other authors define a phasor as a complex sinusoidal quantity with a constant frequency [34].

Define the admittance matrix of the electrical network by

$$\mathcal{Y} := \mathcal{B}\left(R + jX\right)^{-1}\mathcal{B}^{\top} \in \mathbb{C}^{|\mathcal{N}|\times|\mathcal{N}|} \tag{5.14}$$

and

$$\begin{aligned} G_{ii} :=& \Re(\mathcal{Y}_{ii}), \quad B_{ii} := \Im(\mathcal{Y}_{ii}), \\ Y_{ik} :=& G_{ik} + jB_{ik} := -\mathcal{Y}_{ik}, \quad i \neq k. \end{aligned}$$

Moreover, it follows immediately that

$$\mathcal{Y}_{ik} = \begin{cases} 0 & \text{if nodes } i \text{ and } k \text{ are not connected} \\ -(R_l + jX_l)^{-1} & \text{if nodes } i \text{ and } k \text{ are connected by line } l \end{cases}$$

and

$$G_{ii} + jB_{ii} = \sum_{l\sim\mathcal{E}_i}(R_l + jX_l)^{-1},$$

where $\mathcal{E}_i$ denotes the set of edges associated to node i. Inserting (5.10) and (5.11) into (5.13) yields

$$I_{qd} = \operatorname{diag}\left(e^{-j\delta_i}\right)\mathcal{Y}\operatorname{diag}\left(e^{j\delta_i}\right)V_{qd}. \tag{5.15}$$

Recall that V_{qd} and I_{qd} defined in (5.12) are expressed in local dq-coordinates. By making use of (5.9) and (5.14), (5.15) can be written component-wise as

$$\begin{aligned} I_{qd,i} &= I_{q,i} + jI_{d,i}, \\ I_{q,i} &= G_{ii}V_i - \sum_{k\sim\mathcal{N}_i}\left(G_{ik}\cos(\delta_{ik}) + B_{ik}\sin(\delta_{ik})\right)V_k, \\ I_{d,i} &= B_{ii}V_i - \sum_{k\sim\mathcal{N}_i}\left(B_{ik}\cos(\delta_{ik}) - G_{ik}\sin(\delta_{ik})\right)V_k, \end{aligned} \tag{5.16}$$

$i \sim \mathcal{N}$, where, for ease of notation, angle differences are written as $\delta_{ik} := \delta_i - \delta_k$. Furthermore, from Definition 2.11 together with (5.9) and (5.16), the power flows in the network are given by

$$\begin{aligned} P_i &= V_i I_{q,i} = \\ & G_{ii}V_i^2 - \sum_{k\sim\mathcal{N}_i}\left(G_{ik}\cos(\delta_{ik}) + B_{ik}\sin(\delta_{ik})\right)V_kV_i \\ Q_i &= -V_iI_{d,i} \\ &= -B_{ii}V_i^2 + \sum_{k\sim\mathcal{N}_i}\left(B_{ik}\cos(\delta_{ik}) - G_{ik}\sin(\delta_{ik})\right)V_kV_i. \end{aligned} \tag{5.17}$$

The equations (5.17) are the standard power flow equations used in most recent work on microgrid stability analysis, *e.g.*, [88, 83, 2, 69].

Remark 5.5. Note that for any other choices of the transformation angle in local dq-coordinates $V_{d_i} \neq 0$. This is usually the case when modeling SGs, since the angle of the internal machine electromagnetic force (EMF) is in general not known. Then, the equations (5.17) become slightly more involved, see [5, Chapter 9].

Furthermore, in local dq-coordinates, the particular inverter model (5.2), (5.3), is given by

$$\begin{aligned} \gamma_i\dot{\delta}_i = \omega_i - \omega^{\text{com}} &= u_i^{\delta} - \omega^{\text{com}}, \\ \gamma_i\tau_{P_i}\dot{P}_i^m &= -P_i^m + P_i, \\ V_i &= u_i^V, \\ \gamma_i\tau_{P_i}\dot{Q}_i^m &= -Q_i^m + Q_i, \end{aligned} \tag{5.18}$$

with $V_{qd,i} = V_i$ (see (5.9)) and P_i and Q_i given by (5.17).

Recall (5.4) and note that

$$\|\hat{v}_{dq,k}\|_2 = \|\hat{V}_{qd,k}\|_2 = \|V_{qd,k}\|_2 = V_k, \quad k \in \mathcal{N}_\ell.$$

Defining the vectors

$$\begin{aligned} \delta_I :=& \operatorname{col}(\delta_i) \in \mathbb{S}^{|\mathcal{N}_1|},\ V_I := \operatorname{col}(V_i) \in \mathbb{R}_{>0}^{|\mathcal{N}_1|}, \\ u^{\delta} :=& \operatorname{col}(u_i^{\delta}) \in \mathbb{R}^{|\mathcal{N}_1|},\ u^V := \operatorname{col}(u_i^V) \in \mathbb{R}^{|\mathcal{N}_1|}, \\ P_I :=& \operatorname{col}(P_i) \in \mathbb{R}^{|\mathcal{N}_1|},\ Q_I := \operatorname{col}(Q_i) \in \mathbb{R}^{|\mathcal{N}_1|}, \\ P_\ell :=& \operatorname{col}(P_k) \in \mathbb{R}^{|\mathcal{N}_\ell|},\ Q_\ell := \operatorname{col}(Q_k) \in \mathbb{R}^{|\mathcal{N}_\ell|}, \\ P_\ell^* :=& \operatorname{col}(P_k^*(V_k)) \in \mathbb{R}^{|\mathcal{N}_\ell|},\ Q_\ell^* := \operatorname{col}(Q_k^*(V_k)) \in \mathbb{R}^{|\mathcal{N}_\ell|}, \end{aligned}$$

with P_i, P_k, Q_i, and Q_k given by (5.17), as well as the matrix

$$T := \operatorname{diag}(\tau_{P_i}) \in \mathbb{R}^{|\mathcal{N}_1|\times|\mathcal{N}_1|},$$

the system (5.2) - (5.5) can be written equivalently by means of (5.4), (5.18), (5.17) as

$$\begin{aligned} \Gamma\dot{\delta}_I &= u^{\delta} - \omega^{\text{com}}\mathbb{1}_{|\mathcal{N}_1|}, \\ \Gamma T\dot{P}^m &= -P^m + P_I, \\ V_I &= u^V, \\ \Gamma T\dot{Q}^m &= -Q^m + Q_I, \\ \underline{0}_{|\mathcal{N}_\ell|} &= P_\ell - P_\ell^*, \\ \underline{0}_{|\mathcal{N}_\ell|} &= Q_\ell - Q_\ell^*, \end{aligned} \tag{5.19}$$

where the last $2|\mathcal{N}_\ell|$ algebraic equations correspond to the power balances at nodes $k \sim \mathcal{N}_\ell$.

This section has illustrated the main modeling steps and assumptions, which lead from the detailed microgrid model (4.10), (4.11) to the model (5.19), (5.17). The model (5.19), (5.17) is frequently used in the analysis and control design of microgrids [88, 89, 15, 82, 83, 2, 69, 85, 86]. Some of the mentioned work is conducted under additional assumptions such as instantaneous power measurements [88, 2, 69], constant voltage amplitudes [88, 15, 2,

82] or small phase angle differences [89, 85, 86]. In addition, ideal clocks are usually assumed, *i.e.*, $\Gamma = \mathbf{I}_{|\mathcal{N}_1|}$. Furthermore, whenever constant impedance or constant current loads are assumed, the algebraic equations in (5.19), (5.17) can be eliminated by an appropriate network reduction. This process is commonly known as Kron reduction and frequently employed in microgrid and power system studies. For further details on Kron reduction, the reader is referred to [55, 26].

6. Conclusions

The present paper has provided a detailed procedure for the model derivation of a three-phase inverter-based microgrid. In particular, it has been shown how—and under which assumptions—the microgrid models usually used in the literature can be obtained from a significantly more complex model derived from fundamental physical laws. The assumptions invoked in the reduction process are often satisfied in standard applications. Therefore, the reduced model represents a valid approximation and may, hence, be useful for control design and system analysis.

Nevertheless, it is important to note that the model derived in the present paper neglects effects such as asymmetric operation, DC-side dynamics of DG units or line capacitances. These facts have to be kept in mind, when performing microgrid analysis based on the derived model and assessing the results.

In future work, we will investigate the suitability of further modeling techniques, such as dynamic phasors, to describe the dynamics of a microgrid in asymmetric operating conditions. Another subject of future research is the derivation of more detailed load models for microgrid applications.

References

[1] Ackermann, T., Andersson, G., & Söder, L. (2001). Distributed generation: a definition. *Electric power systems research*, *57*, 195–204.

[2] Ainsworth, N., & Grijalva, S. (2013). A structure-preserving model and sufficient condition for frequency synchronization of lossless droop inverter-based AC networks. *IEEE Transactions on Power Systems*, *28*, 4310–4319.

[3] Akagi, H., Kanazawa, Y., & Nabae, A. (1983). Generalized theory of the instantaneous reactive power in three-phase circuits. In *International Power Electronic Conference (IPEC)* (pp. 1375–1386). volume 83.

[4] Akagi, H., Watanabe, E. H., & Aredes, M. (2007). *Instantaneous power theory and applications to power conditioning*. John Wiley & Sons.

[5] Anderson, P., & Fouad, A. (2002). *Power system control and stability*. J.Wiley & Sons.

[6] Andersson, G. (2012). Dynamics and control of electric power systems. *Lecture notes, EEH - Power Systems Laboratory, ETH Zürich*, .

[7] Aredes, M., Akagi, H., Watanabe, E. H., Vergara Salgado, E., & Encarnacao, L. F. (2009). Comparisons between the p–q and p–q–r theories in three-phase four-wire systems. *IEEE Transactions on Power Electronics,*, *24*, 924–933.

[8] Barnes, M., Kondoh, J., Asano, H., Oyarzabal, J., Ventakaramanan, G., Lasseter, R., Hatziargyriou, N., & Green, T. (2007). Real-world microgrids-an overview. In *IEEE Int. Conf. on System of Systems Engineering, 2007. SoSE '07* (pp. 1 –8).

[9] Beck, H.-P., & Hesse, R. (2007). Virtual synchronous machine. In *9th Int. Conf. on Electr. Power Quality and Utilisation.* (pp. 1 –6).

[10] Bidram, A., Davoudi, A., Lewis, F. L., & Qu, Z. (2013). Secondary control of microgrids based on distributed cooperative control of multi-agent systems. *IET Generation, Transmission & Distribution*, *7*, 822–831.

[11] Bidram, A., Lewis, F., & Davoudi, A. (2014). Distributed control systems for small-scale power networks: Using multiagent cooperative control theory. *IEEE Control Systems Magazine*, *34*, 56–77.

[12] Blaabjerg, F., Teodorescu, R., Liserre, M., & Timbus, A. V. (2006). Overview of control and grid synchronization for distributed power generation systems. *IEEE Transactions on Industrial Electronics*, *53*, 1398–1409.

[13] Bolognani, S., Cavraro, G., Carli, R., & Zampieri, S. (2013). A distributed feedback control strategy for optimal reactive power flow with voltage constraints. *arXiv preprint arXiv:1303.7173*, .

[14] Bolognani, S., & Zampieri, S. (2013). A distributed control strategy for reactive power compensation in smart microgrids. *IEEE Transactions on Automatic Control*, *58*, 2818–2833.

[15] Bouattour, H., Simpson-Porco, J. W., Dörfler, F., & Bullo, F. (2013). Further results on distributed secondary control in microgrids. In *52nd Conference on Decision and Control* (pp. 1514–1519).

[16] Buchholz, F. (1950). *Das Begriffssystem Rechtleistung, Wirkleistung, totale Blindleistung*. Selbstverl.;[Lachner in Komm].

[17] Chandorkar, M., Divan, D., & Adapa, R. (1993). Control of parallel connected inverters in standalone AC supply systems. *IEEE Transactions on Industry Applications*, *29*, 136 –143.

[18] Chiniforoosh, S., Jatskevich, J., Yazdani, A., Sood, V., Dinavahi, V., Martinez, J., & Ramirez, A. (2010). Definitions and applications of dynamic average models for analysis of power systems. *IEEE Transactions on Power Delivery*, *25*, 2655–2669.

[19] Chowdhury, S., & Crossley, P. (2009). *Microgrids and active distribution networks*. The Institution of Engineering and Technology.

[20] Coelho, E., Cortizo, P., & Garcia, P. (2002). Small-signal stability for parallel-connected inverters in stand-alone AC supply systems. *IEEE Transactions on Industry Applications*, *38*, 533 –542.

[21] Depenbrock, M. (1962). *Untersuchungen über die Spannungs- und Leistungsverhältnisse bei Umrichtern ohne Energiespeicher*. Ph.D. thesis Mikrokopie GmbH.

[22] Depenbrock, M. (1993). The FBD-method, a generally applicable tool for analyzing power relations. *IEEE Transactions on Power Systems*, *8*, 381–387.

[23] Depenbrock, M., Staudt, V., & Wrede, H. (2004). Concerning" instantaneous power compensation in three-phase systems by using pqr theory". *IEEE Transactions on Power Electronics*, *19*, 1151–1152.

[24] Dhople, S. V., Johnson, B. B., Dörfler, F., & Hamadeh, A. O. (2014). Synchronization of nonlinear circuits in dynamic electrical networks with general topologies. *IEEE Transactions on Circuits and Systems I: Regular Papers*, *61*, 2677–2690.

[25] DIN 40110-1:1994 (1994). DIN 40110-1:1994 - Wechselstromgrößen; Zweileiter-Stromkreise, (engl: "Quantities used in alternating current theory; two-line circuits).

[26] Dörfler, F., & Bullo, F. (2013). Kron reduction of graphs with applications to electrical networks. *IEEE Transactions on Circuits and Systems I: Regular Papers*, *60*, 150–163.

[27] Dörfler, F., Bullo, F. et al. (2014). Breaking the hierarchy: Distributed control & economic optimality in microgrids. *arXiv preprint arXiv:1401.1767*, .

[28] Emanuel, A. E. (2004). Summary of ieee standard 1459: definitions for the measurement of electric power quantities under sinusoidal, nonsinusoidal, balanced, or unbalanced conditions. *IEEE Transactions on Industry Applications*, *40*, 869–876.

[29] Erickson, R. W., & Maksimovic, D. (2001). *Fundamentals of power electronics*. Springer.

[30] Farhangi, H. (2010). The path of the smart grid. *IEEE Power and Energy Magazine*, *8*, 18 –28.

[31] Fiaz, S., Zonetti, D., Ortega, R., Scherpen, J., & van der Schaft, A. (2013). A port-hamiltonian approach to power network modeling and analysis. *European Journal of Control*, *19*, 477–485.

[32] Fryze, S. (1932). Wirk-, Blind-und Scheinleistung in elektrischen Stromkreisen mit nichtsinusförmigem Verlauf von Strom und Spannung. *Elektrotechnische Zeitschrift*, *25*, 569–599.

[33] Fukuda, S., & Yoda, T. (2001). A novel current-tracking method for active filters based on a sinusoidal internal model [for pwm invertors]. *IEEE Transactions on Industry Applications*, *37*, 888–895.

[34] Glover, J. D., Sarma, M. S., & Overbye, T. J. (2011). *Power system analysis and design*. Cengage Learning.

[35] Godsil, C., & Royle, G. (2001). *Algebraic graph theory*. Springer.

[36] Grainger, J. J., & Stevenson, W. D. (1994). *Power system analysis* volume 621. McGraw-Hill New York.

[37] Green, T., & Prodanovic, M. (2007). Control of inverter-based micro-grids. *Electric Power Systems Research*, *Vol. 77*, 1204–1213.

[38] Guerrero, J., Loh, P., Chandorkar, M., & Lee, T. (2013). Advanced control architectures for intelligent microgrids – part I: Decentralized and hierarchical control. *IEEE Transactions on Industrial Electronics*, *60*, 1254–1262.

[39] Guerrero, J., Vasquez, J., Matas, J., de Vicuna, L., & Castilla, M. (2011). Hierarchical control of droop-controlled AC and DC microgrids; a general approach toward standardization. *IEEE Transactions on Industrial Electronics*, *58*, 158 –172.

[40] Guo, Y., & Gawlik, W. (). A survey of control strategies applied in worldwide microgrid projects. *Tagungsband ComForEn 2014*, (p. 47).

[41] Hans, C. A., Nenchev, V., Raisch, J., & Reincke-Collon, C. (2014). Minimax model predictive operation control of microgrids. To appear at 19th IFAC World Congress, Cape Town, South Africa.

[42] Hansen, J., Sato, M., Ruedy, R., Nazarenko, L., Lacis, A., Schmidt, G., Russell, G., Aleinov, I., Bauer, M., Bauer, S. et al. (2005). Efficacy of climate forcings. *Journal of Geophysical Research: Atmospheres (1984–2012)*, *110*.

[43] Hatziargyriou, N., Asano, H., Iravani, R., & Marnay, C. (2007). Microgrids. *IEEE Power and Energy Magazine*, *5*, 78–94.

[44] Hazewinkel, M. (1993). *Encyclopaedia of Mathematics (9)* volume 9. Springer.

[45] Heuck, K., Dettmann, K.-D., & Schulz, D. (2013). *Elektrische Energieversorgung: Erzeugung, Übertragung und Verteilung elektrischer Energie für Studium und Praxis*. Springer DE.

[46] Hornik, T., & Zhong, Q.-C. (2011). A current-control strategy for voltage-source inverters in microgrids based on and repetitive control. *IEEE Transactions on Power Electronics*, *26*, 943–952.

[47] Houghton, J. T. (1996). *Climate change 1995: The science of climate change: contribution of working group I to the second assessment report of the Intergovernmental Panel on Climate Change* volume 2. Cambridge University Press.

[48] Justo, J. J., Mwasilu, F., Lee, J., & Jung, J.-W. (2013). Ac-microgrids versus dc-microgrids with distributed energy resources: A review. *Renewable and Sustainable Energy Reviews*, *24*, 387–405.

[49] Katiraei, F., & Iravani, M. (2006). Power management strategies for a microgrid with multiple distributed generation units. *IEEE Transactions on Power Systems*, *21*, 1821 –1831.

[50] Katiraei, F., Iravani, M., & Lehn, P. (2007). Small-signal dynamic model of a micro-grid including conventional and electronically interfaced distributed resources. *IET Generation, Transmission Distribution*, *1*, 369–378.

[51] Katiraei, F., Iravani, R., Hatziargyriou, N., & Dimeas, A. (2008). Microgrids management. *IEEE Power and Energy Magazine*, *6*, 54–65.

[52] Khalil, H. K. (2002). *Nonlinear systems* volume 3. Prentice Hall.

[53] Kim, H., & Akagi, H. (1999). The instantaneous power theory on the rotating pqr reference frames. In *International Conference on Power Electronics and Drive Systems (PEDS)* (pp. 422–427). IEEE volume 1.

[54] Kokotovic, P., Khali, H. K., & O'reilly, J. (1999). *Singular perturbation methods in control: analysis and design* volume 25. Siam.

[55] Kundur, P. (1994). *Power system stability and control*. McGraw-Hill.

[56] Kwasinski, A., & Onwuchekwa, C. N. (2011). Dynamic behavior and stabilization of DC microgrids with instantaneous constant-power loads. *IEEE Transactions on Power Electronics*, *26*, 822–834.

[57] Lasseter, R. (2002). Microgrids. In *IEEE Power Engineering Society Winter Meeting, 2002* (pp. 305 – 308 vol.1). volume 1.

[58] Lasseter, R. H. (2011). Smart distribution: Coupled microgrids. *Proceedings of the IEEE*, *99*, 1074–1082.

[59] Lidula, N., & Rajapakse, A. (2011). Microgrids research: A review of experimental microgrids and test systems. *Renewable and Sustainable Energy Reviews*, *15*, 186–202.

[60] Loh, P. C., & Holmes, D. G. (2005). Analysis of multiloop control strategies for LC/CL/LCL-filtered voltage-source and current-source inverters. *IEEE Transactions on Industry Applications*, *41*, 644–654.

[61] Lopes, J., Moreira, C., & Madureira, A. (2006). Defining control strategies for microgrids islanded operation. *IEEE Transactions on Power Systems*, *21*, 916 – 924.

[62] Luo, L., & Dhople, S. (2014). Spatiotemporal model reduction of inverter-based islanded microgrids. *IEEE Transactions on Energy Conversion*, *29*, 823–832.

[63] Machowski, J., Bialek, J., & Bumby, J. (2008). *Power system dynamics: stability and control*. J.Wiley & Sons.

[64] Mariani, V., Vasca, F., & Guerrero, J. M. (2014). Analysis of droop controlled parallel inverters in islanded microgrids. In *IEEE International Energy Conference (ENERGYCON)* (pp. 1304–1309). IEEE.

[65] Mariani, V., Vasca, F., & Guerrero, J. M. (2014). Dynamic-phasor-based nonlinear modelling of AC islanded microgrids under droop control. In *11th International Multi-Conference on Systems, Signals & Devices (SSD)* (pp. 1–6). IEEE.

[66] Miao, Z., Domijan, A., & Fan, L. (2011). Investigation of microgrids with both inverter interfaced and direct AC-connected distributed energy resources. *IEEE Transactions on Power Delivery*, *26*, 1634 –1642.

[67] Mohamed, Y., & El-Saadany, E. (2008). Adaptive decentralized droop controller to preserve power sharing stability of paralleled inverters in distributed generation microgrids. *IEEE Transactions on Power Electronics*, *23*, 2806 –2816.

[68] Mohan, N., & Undeland, T. M. (2007). *Power electronics: converters, applications, and design*. John Wiley & Sons.

[69] Münz, U., & Metzger, M. (2014). Voltage and angle stability reserve of power systems with renewable generation. In *19th IFAC World Congress* (pp. 9075–9080). Cape Town, South Africa.

[70] Paap, G. C. (2000). Symmetrical components in the time domain and their application to power network calculations. *IEEE Transactions on Power Systems*, *15*, 522–528.

[71] Park, R. H. (1929). Two-reaction theory of synchronous machines generalized method of analysis-part I. *Transactions of the American Institute of Electrical Engineers*, *48*, 716–727.

[72] Peng, F. Z., & Lai, J.-S. (1996). Generalized instantaneous reactive power theory for three-phase power systems. *IEEE*

Transactions on Instrumentation and Measurement, *45*, 293–297.

[73] Planas, E., Gil-de Muro, A., Andreu, J., Kortabarria, I., & Martínez de Alegría, I. (2013). General aspects, hierarchical controls and droop methods in microgrids: A review. *Renewable and Sustainable Energy Reviews*, *17*, 147–159.

[74] Pogaku, N., Prodanovic, M., & Green, T. (2007). Modeling, analysis and testing of autonomous operation of an inverter-based microgrid. *IEEE Transactions on Power Electronics*, *22*, 613 –625.

[75] Prodanovic, M., & Green, T. C. (2003). Control and filter design of three-phase inverters for high power quality grid connection. *IEEE Transactions on Power Electronics*, *18*, 373–380.

[76] Riverso, S., Sarzo, F., & Ferrari-Trecate, G. (2014). Plug-and-play voltage and frequency control of islanded microgrids with meshed topology. *arXiv preprint arXiv:1405.2421*, .

[77] Rocabert, J., Luna, A., Blaabjerg, F., & Rodriguez, P. (2012). Control of power converters in AC microgrids. *IEEE Transactions on Power Electronics*, *27*, 4734–4749.

[78] Salomonsson, D. (2008). *Modeling, Control and Protection of Low-Voltage DC Microgrids*. Ph.D. thesis KTH, Electric Power Systems.

[79] Salomonsson, D., Soder, L., & Sannino, A. (2009). Protection of low-voltage dc microgrids. *IEEE Transactions on Power Delivery*, *24*, 1045–1053.

[80] Sauer, P., & Pai, M. (1998). *Power system dynamics and stability*. Prentice Hall.

[81] Schiffer, J., Anta, A., Trung, T. D., Raisch, J., & Sezi, T. (2012). On power sharing and stability in autonomous inverter-based microgrids. In *51st Conference on Decision and Control* (pp. 1105–1110). Maui, HI, USA.

[82] Schiffer, J., Goldin, D., Raisch, J., & Sezi, T. (2013). Synchronization of droop-controlled microgrids with distributed rotational and electronic generation. In *52nd Conference on Decision and Control* (pp. 2334–2339). Florence, Italy.

[83] Schiffer, J., Ortega, R., Astolfi, A., Raisch, J., & Sezi, T. (2014). Conditions for stability of droop-controlled inverter-based microgrids. *Automatica*, *50*, 2457–2469.

[84] Schiffer, J., Ortega, R., Hans, C., & Raisch, J. (2015). Droop-controlled inverter-based microgrids are robust to clock drifts. *American Control Conference*, . To appear.

[85] Schiffer, J., Seel, T., Raisch, J., & Sezi, T. (2014). A consensus-based distributed voltage control for reactive power sharing in microgrids. In *13th European Control Conference* (pp. 1299–1305). Strasbourg, France.

[86] Schiffer, J., Seel, T., Raisch, J., & Sezi, T. (2014). Voltage stability and reactive power sharing in inverter-based microgrids with consensus-based distributed voltage control. *IEEE Transactions on Control Systems Technology*, . Submitted.

[87] Shafiee, Q., Guerrero, J., & Vasquez, J. (2014). Distributed secondary control for islanded microgrids – a novel approach. *IEEE Transactions on Power Electronics*, *29*, 1018–1031.

[88] Simpson-Porco, J. W., Dörfler, F., & Bullo, F. (2013). Synchronization and power sharing for droop-controlled inverters in islanded microgrids. *Automatica*, *49*, 2603 – 2611.

[89] Simpson-Porco, J. W., Dörfler, F., & Bullo, F. (2013). Voltage stabilization in microgrids using quadratic droop control. In *52nd Conference on Decision and Control* (pp. 7582–7589). Florence, Italy.

[90] Solomon, S. (2007). *Climate change 2007-the physical science basis: Working group I contribution to the fourth assessment report of the IPCC* volume 4. Cambridge University Press.

[91] Teodorescu, R., Blaabjerg, F., Liserre, M., & Loh, P. C. (2006). Proportional-resonant controllers and filters for grid-connected voltage-source converters. *IEE Proceedings-Electric Power Applications*, *153*, 750–762.

[92] Teodorescu, R., Liserre, M., & Rodriguez, P. (2011). *Grid converters for photovoltaic and wind power systems* volume 29. John Wiley & Sons.

[93] Tôrres, L., Hespanha, J. P., & Moehlis, J. (2013). Synchronization of oscillators coupled through a network with dynamics: A constructive approach with applications to the parallel operation of voltage power supplies. *IEEE Transactions on Automatic Control. Current status: under review*, .

[94] Van Cutsem, T., & Vournas, C. (1998). *Voltage stability of electric power systems* volume 441. Springer.

[95] Varaiya, P. P., Wu, F. F., & Bialek, J. W. (2011). Smart operation of smart grid: Risk-limiting dispatch. *Proceedings of the IEEE*, *99*, 40–57.

[96] Venkatasubramanian, V., Schattler, H., & Zaborszky, J. (1995). Fast time-varying phasor analysis in the balanced three-phase large electric power system. *IEEE Transactions on Automatic Control*, *40*, 1975–1982.

[97] Visscher, K., & De Haan, S. (2008). Virtual synchronous machines for frequency stabilisation in future grids with a significant share of decentralized generation. In *SmartGrids for Distribution, 2008. IET-CIRED. CIRED Seminar* (pp. 1 –4).

[98] Wang, X., Guerrero, J. M., Blaabjerg, F., & Chen, Z. (2012). A review of power electronics based microgrids. *Journal of Power Electronics*, *12*, 181–192.

[99] Weiss, G., Zhong, Q.-C., Green, T. C., & Liang, J. (2004). $H\infty$ repetitive control of DC-AC converters in microgrids. *IEEE Transactions on Power Electronics*, *19*, 219–230.

[100] Willems, J. L. (1992). A new interpretation of the akagi-nabae power components for nonsinusoidal three-phase situations. *IEEE Transactions on Instrumentation and Measurement*, *41*, 523–527.

[101] Willems, J. L., Ghijselen, J. A., & Emanuel, A. E. (2005). The apparent power concept and the IEEE standard 1459-2000. *IEEE Transactions on Power Delivery*, *20*, 876–884.

[102] Zhong, Q., & Weiss, G. (2011). Synchronverters: Inverters that mimic synchronous generators. *IEEE Transactions on Industrial Electronics*, *58*, 1259 –1267.

[103] Zhong, Q.-C., & Hornik, T. (2012). *Control of power inverters in renewable energy and smart grid integration*. John Wiley & Sons.